REPORT FHWA/NY/SR-06/148

MONITORING AND STRUCTURAL INTEGRITY EVALUATION OF COEYMANS CREEK BRIDGE FOR SUPERLOAD CROSSING

OSMAN HAG-ELSAFI
JONATHAN KUNIN

SPECIAL REPORT 148
TRANSPORTATION RESEARCH AND DEVELOPMENT BUREAU
New York State Department of Transportation
George E. Pataki, Governor/Thomas J. Madison Jr., Commissioner

Monitoring and Structural Integrity Evaluation of Coeymans Creek Bridge for Superload Crossing

Osman Hag-Elsafi, Engineering Research Specialist I
Jonathan Kunin, Civil Engineer I

Conducted in Cooperation With
The U.S. Department of Transportation
Federal Highway Administration

Special Report 148
July 2006

TRANSPORTATION RESEARCH AND DEVELOPMENT BUREAU
New York State Department of Transportation, 50 Wolf Road, Albany, NY 12232

ABSTRACT

Monitoring and structural integrity evaluation of Coeymans Creek Bridge for superload permit trucks are discussed in this report. The superloads were boiler modules carried on 16-axle trailers, driven by one or two tractors/power units during the bridge crossing. The bridge is an integral abutment structure consisting of eleven prestressed concrete box-beams with a composite concrete deck. Approval of the superload permits was based on an engineering analysis, which recommended crossing of the bridge in two configurations. The first, required a crabbed trailer be towed across the bridge and the second, called for a trailer be driven in a diagonal crossing fashion. Crabbing, steering a trailer wheels to remain parallel to the bridge centerline during the crossing, was recommended for moves of gross weights exceeding 1775 kN (400 kips) and diagonal crossing was recommended for those lighter than 1775 kN (400 kips). The low rating of the structure and the unusually heavy loads motivated the need for investigating actual stress levels in the bridge beams during the superload moves. There was also interest in comparing the two recommended crossing patterns and investigating the level of fixity provided by the integral abutments. The beams were instrumented and strain data was collected during four of the moves. Analysis of the collected data indicated that the stresses in the beams remained below that which would have caused cracking and that, for this bridge, crabbing had no clear benefits over diagonal crossing. The analysis also indicated that the bridge has good transverse load distribution and a significant level of end fixity provided by the integral abutments.

Additional load testing was conducted using two dump trucks loaded with sand. The testing included crossing the structure in two configurations, at six designated locations on the deck. The objective of the testing was to investigate the behavior of the structure due to trucks crossing in a straight fashion, and study how this behavior compares to that due to the superloads. The results from the monitoring and testing indicated that the highest load distribution on the beams remained the same (about 14 percent), regardless of the magnitude of the load on the bridge or the crossing pattern.

CONTENTS

I. INTRODUCTION

A. BACKGROUND

Transportation agencies sometimes receive permit requests for superloads, unusually heavy loads, to cross bridges on specified highway routes *(1-5)*. Before a decision is made, the agencies receiving these requests, often investigate the capacity of impacted bridges along requested travel routes, to ensure the structural integrity and safety of these bridges during crossing of the transported loads *(1-3, 6, 7)*. Turner and Aktan monitored and modeled three steel stringer bridges in Ohio for a 3300 kN (371-ton) superload. Any structural damage to the bridge would be compensated, if the damage could be documented. In addition to monitoring for damage, their investigation found that a combination of field testing and finite element modeling could predict a structure's response to a superload. This information would assist engineers in optimizing axle configurations and crossing patterns. Hunt and Helmicki monitored several superloads, including one weighing over 3927 kN (883-kips), crossing a 6-span, 198-m (650-ft) long steel girder bridge. Truckload experiments were conducted to generate a strain influence line for the structure. Using the generated influence line, the authors were able to predict actual stresses induced by the superloads. Truckload experiments performed after a superload crossing were able to detect damage, and assess the effect on the bridge's integrity. Coeymans Creek Bridge was one of the structures in the requested transport route for the four superloads discussed in this report.

B. COEYMANS CREEK BRIDGE

The bridge (BIN 1007560) carries State Route 9W over Coeymans Creek near the Town of Coeymans, South of Albany, NY. The bridge is a single span, integral abutment structure built in 1985. It consists of eleven 32.6-m (107.5-ft) long, adjacent prestressed concrete box beams and a 15.2-cm (6-in.) thick composite concrete deck. The 3 most interior (center) beams are 0.91-m (3-ft) wide and the remaining 8 exterior beams are 1.22-m (4-ft) wide. The interior and exterior beams [standard 107-cm (42-in) deep AASHTO box beams] were respectively prestressed using 34 and 42, 1862 MPa (270 ksi) 13 mm (1/2 in) strands. The inventory and operating ratings of the bridge are 33.5 and 86.1 metric tons (36.9 and 87.2 tons), respectively *(7, 8)*. The condition of the deck is rated a 5 on a scale 0 to 9, signifying a fair condition with visible longitudinal cracking. The bridge span is 33.02-m (107-ft) long, and has 2 lanes of traffic. The annual average daily traffic is about 9197 vehicles. A photo and a plan view of the bridge are shown in Figures 1 and 2, respectively, and bridge beam sections in Figure 3.

Figure 1. Coeymans Creek Bridge.

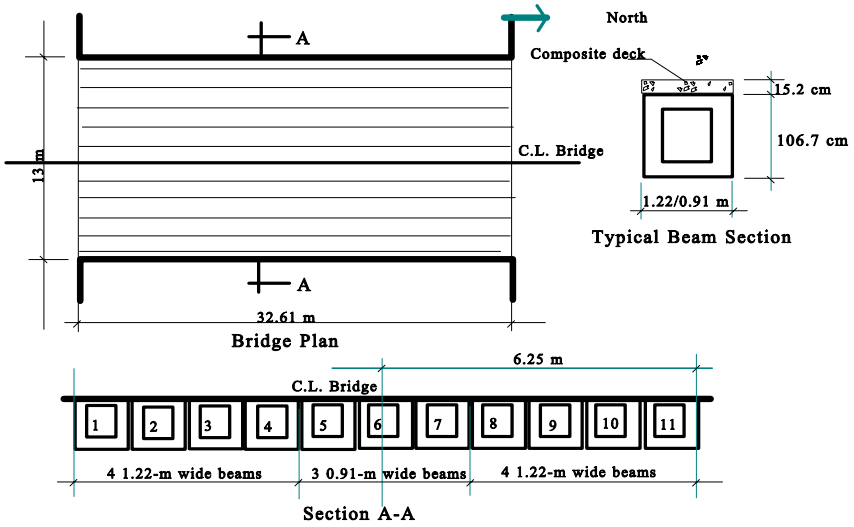

Figure 2. Bridge plan (Not to scale).

C. OBJECTIVES

The bridge beams were instrumented with strain gages to monitor the superload moves as they cross the bridge at a crawl speed. The main objective of the monitoring was to measure the actual stress levels in the beams and determine whether the bridge integrity was compromised during the moves or not. Two additional objectives of the monitoring were to study the two crossing patterns to identify the merits of one over the other, if any, and to produce information about the level of fixity provided by the integral abutments. Additional load testing was conducted using two dump trucks loaded with sand. The objectives of the testing were to investigate the behavior of the structure due to trucks crossing in a straight fashion, and study how this behavior compares to that due to the superloads. Such information could be helpful in making educated decisions for similar future moves. The major contribution of this study is that it is the first of its kind to compare the two crossing patterns and monitor a prestreesed concrete integral abutment structure for superloads.

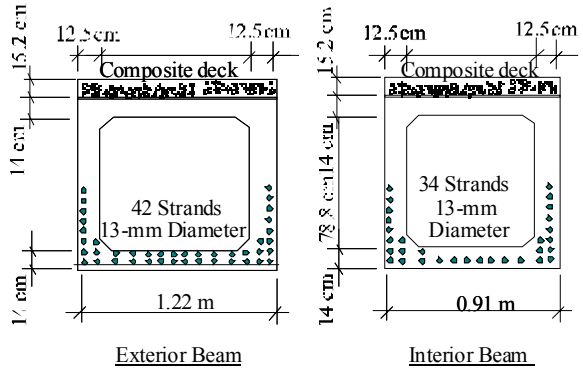

Figure 3. Beam sections (Not to scale).

D. REPORT ORGANIZATION

In the next chapter, the monitored superload and crossing patterns are described. Plans for instrumentation, monitoring, and load testing of the bridge are discussed in Chapter 3. Results from the superload monitoring are presented and discussed in Chapter 4. Chapter 5 includes results and discussions of the load tests, as well as comparison of these results with those obtained from the superload monitoring. Conclusions from the study are presented in the final chapter of the report.

II. SUPERLOADS AND CROSSING PATTERNS

A. SUPERLOADS

The superloads, boiler modules, ranging in weight from 369 to1125 kN (83 to 253 kips), were carried on 16-axle trailers each weighing about 547 kN (123 kips). The trailers carrying the heavier modules were towed in a crabbed configuration across the bridge by two, 4-axle tractors/power units, each weighing about 205 kN (46 kips). Those carrying lighter modules crossed the bridge diagonally, driven by a single 3-axle tractor/power unit weighing approximately 342 kN (77 kips). Photos of a loaded trailer and driving power units are shown in Figures 4 and 5, respectively.

Figure 4. A loaded trailer.

Figure 5. Driving power units.

B. CROSSING PATTERNS

The first and third superload moves, with gross weights (weight of tractors, boiler module, and trailer) of 2028 kN (455 kips) and 2015 kN (452 kips), respectively, crossed the bridge in a crabbed configuration. In this configuration, the trailer is positioned as in Figure 6 with the wheels steered to cross the structure parallel to the bridge centerline. The second and fourth superload moves, with gross weight (weight of tractors, boiler module, and trailer) of 1205 kN (270 kips) 1260 kN (282 kips), respectively, crossed the bridge diagonally. In a diagonal crossing configuration, the trailer carrying the load is driven diagonally across the bridge, with the wheels free as shown in Figure 7. The first and second superloads crossed on January 28, 2002, and the third and fourth on March 06, 2002. A summary of the superloads information data is given in Table 1.

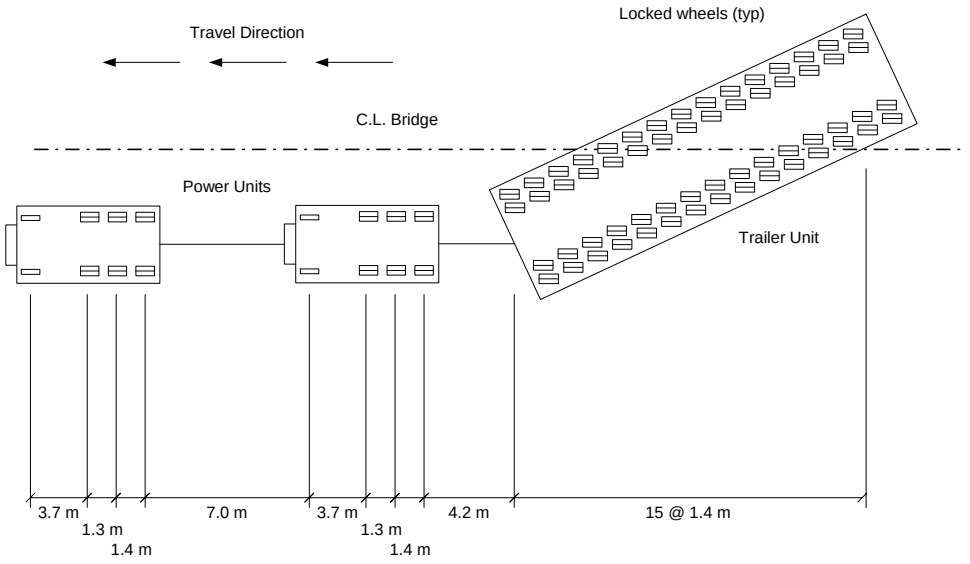

Figure 6. A superload crossing in a crabbed configuration (Not to scale).

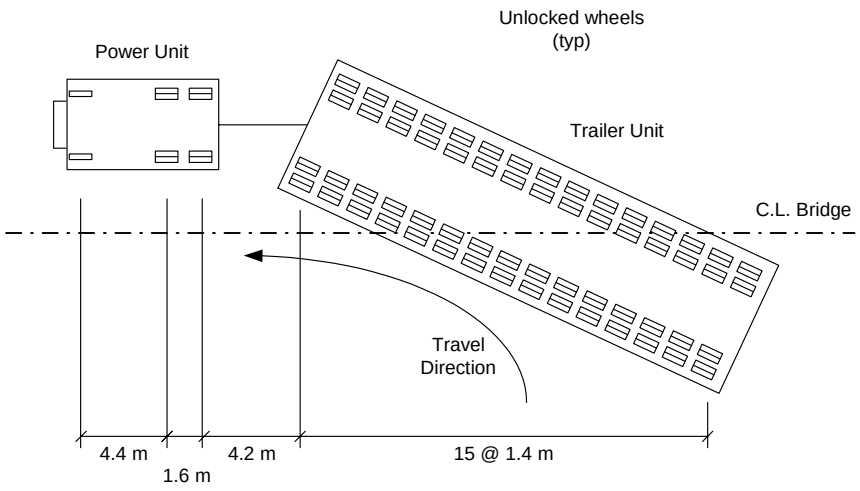

Figure 7. A superload crossing diagonally (Not to scale).

Superload Designation	Date Crossed	Gross Weight	Crossing Pattern
First	January 28, 2002	2028 kN (456 kip)	Crabbed
Second	January 28, 2002	1205 kN (271 kip)	Diagonal
Third	March 6, 2002	2015 kN (453 kip)	Crabbed
Fourth	March 6, 2002	1260 kN (282 kip)	Diagonal

Table 1. Superload trucks information data.

III. INSTRUMENTATION, MONITORING, AND LOAD TESTING

The bridge instrumentation and superload monitoring are discussed in this chapter. In order to investigate the bridge behaviour under normal traffic loading, additional plans were made to test the bridge using two trucks of known weights and configurations crossing in a straight fashion, parallel to the bridge center line. These additional tests are also discussed in this chapter.

A. INSTRUMENTATION

The bridge was instrumented at various locations on the beams to determine 1) maximum stresses in the beams, 2) transverse load distribution, 3) neutral axis location in a fascia beam, and 4) fixity at both ends of Beam 8 at the abutments.

The bridge beams were numbered, sequentially, Beams 1 to 11, starting with the westside fascia beam. BDI gages (manufactured by Bridge Diagnostics, Inc.) were mounted at the midspans of nine of the eleven beams (Beams 1, 3, and 5-11). Two more gages were also mounted on the exposed side of Beam 11, a fascia beam, to provide data for locating the neutral axis. Additional gages were also mounted on Beam 8 to investigate fixity at the integral abutments. The instrumentation plan is shown in Figure 8. A general purpose strain gage measurement system (the "System 6000" manufactured by the Measurement Group) was employed for data acquisition.

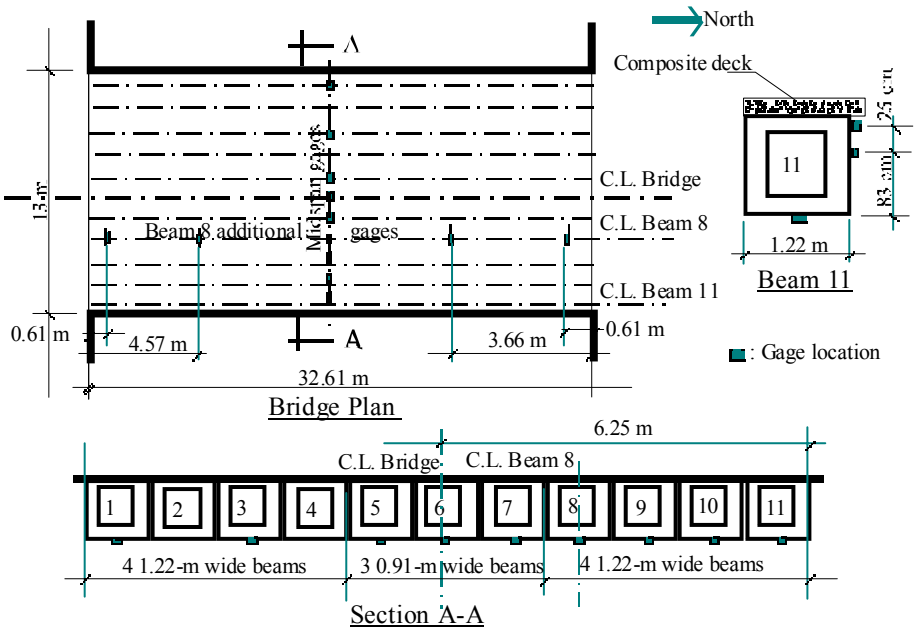

Figure 8. Instrumentation plan (Not to scale).

A Mathcad program was developed to determine axle locations (on or off the bridge) and moments and shear forces at any time during a superload crossing. The program input includes the bridge span length, axle configurations and weights, the times the first axle entered and the last axle exited the bridge, a location along the span where moment and shear force are to be evaluated, and the instant in time the evaluation is desired. The program uses the axle locations and weights to calculate the moments and shear forces, assuming both simply supported and fixed-ends conditions. The program output includes axle locations on the bridge, midspan and end moments, and shear forces for both simply supported and fixed-ends conditions, and the moment and shear force at the selected location for evaluation. The program was useful in determining midspan moments, assuming simply supported or completely fixed end conditions for comparison with those based on monitored strain data.

B. MONITORING

Monitoring strain data was collected at a frequency of 100 samples per second, during each of the superload crossings. During a crossing, the bridge was cleared of all traffic and the superload was moved at a speed of approximately 8 km/hour (5 miles/hour) (crawl speed). Strain data was collected continuously during each crossing; starting and ending a few seconds before and after a load entered and exited the bridge. The bridge inspection reports were obtained and a visual inspection for damage was conducted at the end of the monitoring program.

C. LOAD TESTING

On March 28, 2002, six load tests were conducted using two of the Department's dump trucks loaded with sand. The test trucks had gross weights of 186 kN (41.9 kips) and 207 kN (46.5 kips). Each of the vehicles used in the load tests closely resembled an AASHTO M-18 (H-20) loading. Truck configurations and axle weights are shown in Figure 9, and additional information on the trucks is given in Table 2.

All six load tests were conducted using the two trucks in straight crossing fashion. In the first five load tests, the test trucks mimicked the superload trucks in the direction of travel (entering from the North end and exiting from the South end of the bridge) and travel speed [crossing at crawl speed (8 km/hr) (5 mph)]. In Load Tests 1 to 4, the two trucks followed each other closely (the second vehicle tailgated the first vehicle) with a wheel line directly positioned on a specific beam in each case (Beams 3, 9, 8, and 4, respectively). In Load Test 5, the two vehicles crossed the bridge in a side by side configuration, with the wheel lines positioned on the centerlines of Beams 3 and 9. The final load test (Load Test 6) was a static test, where the two vehicles were positioned with the wheel lines centered on Beams 3 and 9 (similar to Load Test 5), and the rear axle of each truck positioned at the bridge midspan. The truck positions during the six load tests are shown in Figure 10.

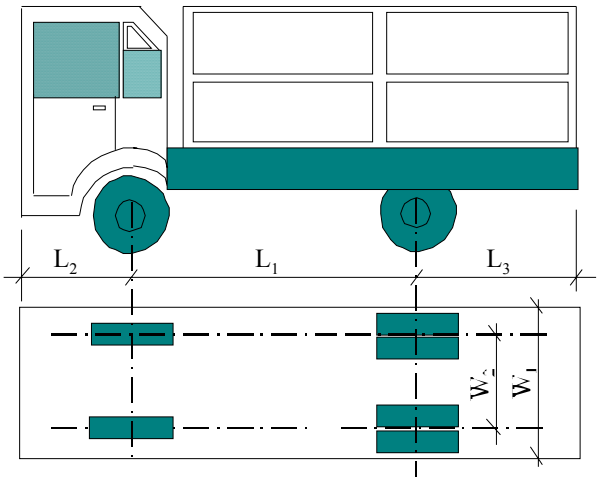

Truck	Length Dimensions (m)			Width Dimensions (m)	
	L_1	L_2	L_3	W_1	W_2
A	4.57	4.85	2.36	2.62	1.96
B	4.57	2.97	2.00	2.62	19.56

Truck	Front Axle (kN)		Back Axle (kN)		Gross Weight (kN)
	Left	Right	Left	Right	
A	33.81	43.33	54.53	54.53	186.20
B	37.54	41.99	63.70	63.70	206.93

Figure 9. Load test trucks (Not to scale).

Truck Type	Date Crossed	Gross Weight	Crossing Pattern
Load Test Vehicles	March 28, 2002 (Load Tests 1-6)	393 kN (88 kip)	Straight

Table 2. Load test trucks information data.

Load Test 1: Crawl Speed

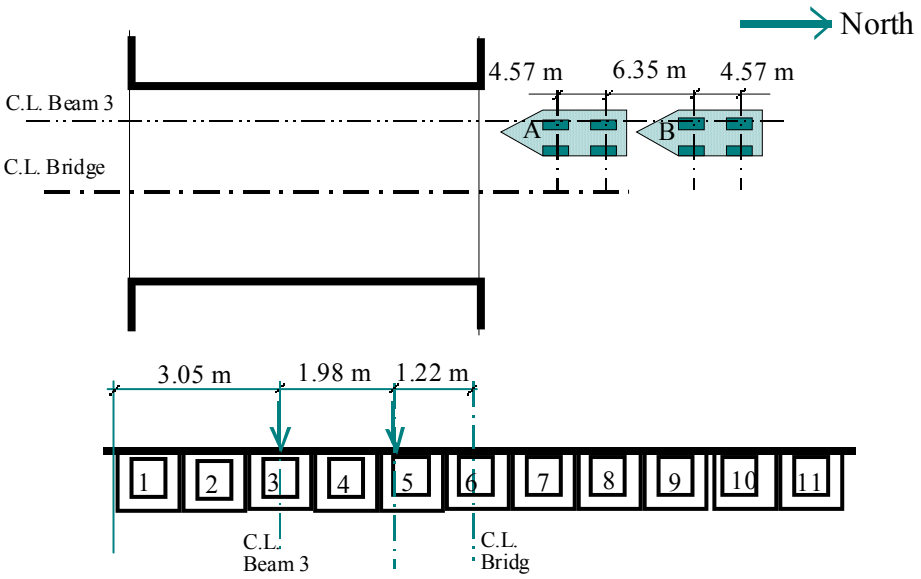

Load Test 2: Crawl Speed

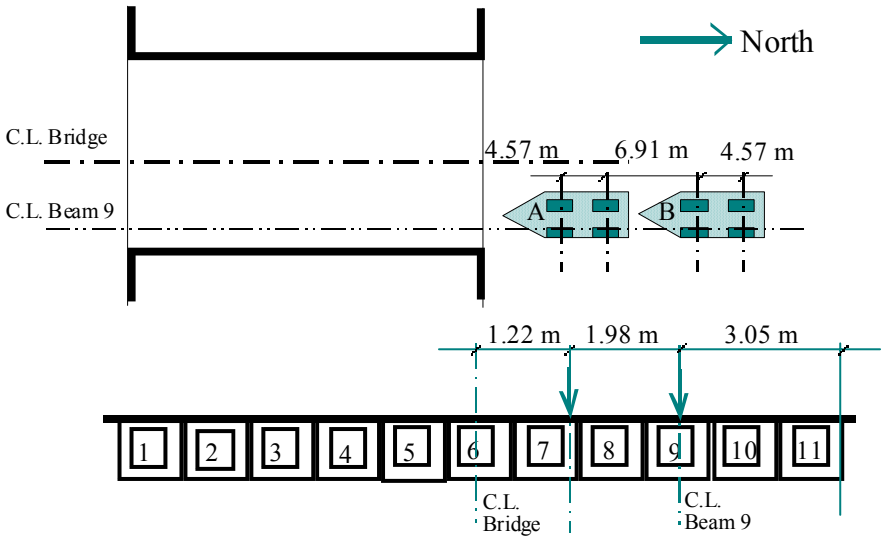

Figure 10. Test truck load casess. Not to scale.

Load Test 3: Crawl Speed

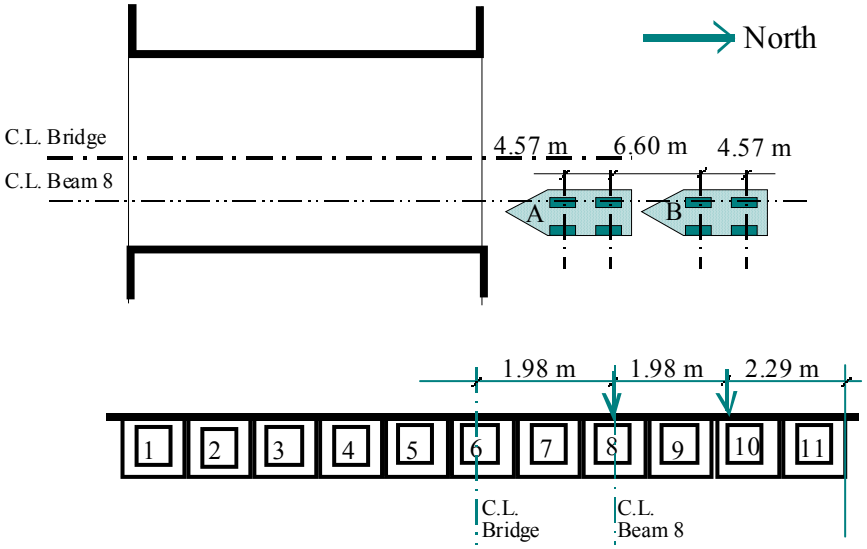

Load Test 4: Crawl Speed

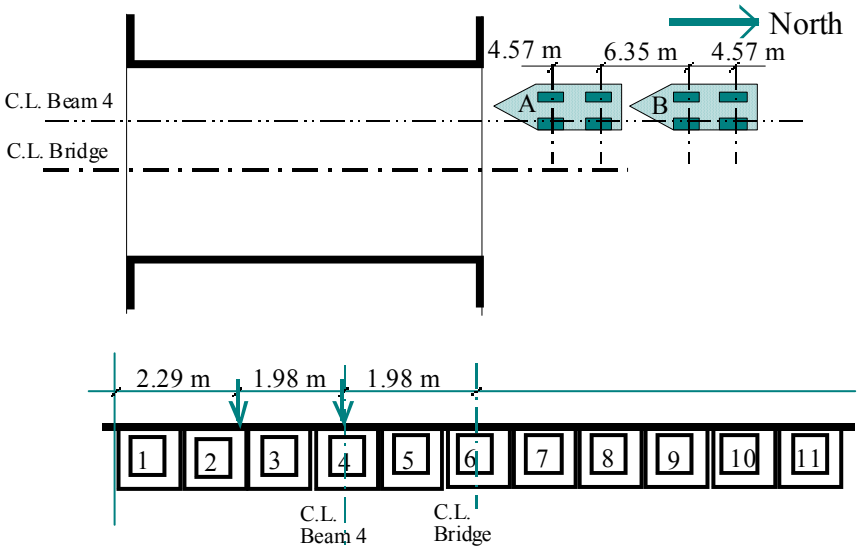

Figure 10. Test truck load cases. Not to scale. (Continued).

Load Test 5: Crawl Speed

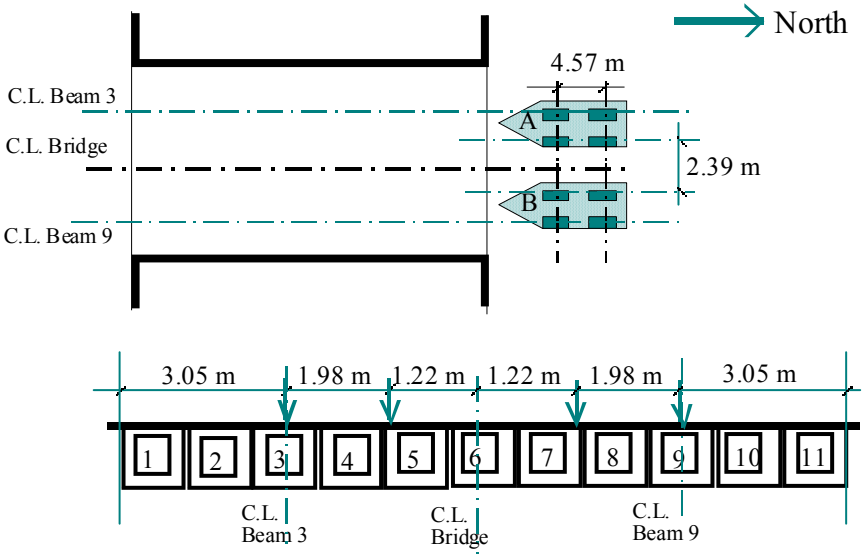

Load Test 6: Static

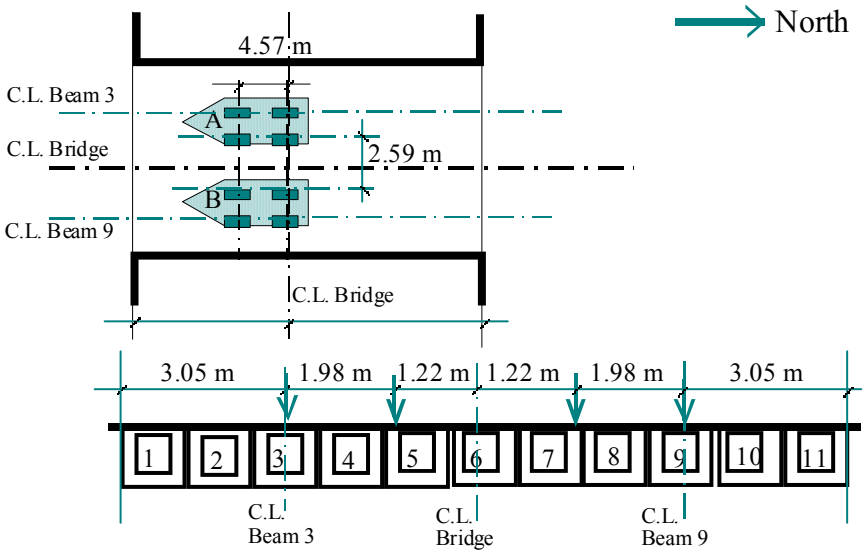

Figure 10. Test truck load cases. Not to scale. (Continued).

IV. SUPERLOAD MONITORING RESULTS

A. STRAIN HISTORIES

Recorded strain results at the midspans of the bridge beams during crossing of the first and second superloads are shown in Figures 11a and 11b, respectively. The highest strains recorded for the first superload was 90 με and for the second was 56 με. Using the developed program, the times corresponding to the maximum strains in the figures were determined to coincide with the instances when a loaded trailer in each case was centered about the bridge midspan. The ratio between these strains (about 1.6) is very close to that between the weights of the loaded trailers for the two superloads (about 1.8). This implies that, when the strains were maximum, the trailers in the two crossing configurations assumed a similar orientation at the bridge midspan (about 22 degrees with the bridge centerline). Thus, it can be concluded that if the crabbed trailer, carrying the first superload, was driven diagonally, similar to the second superload, its midspan strain plot would be very close to that in Figure 11a. This conclusion is also supported by the similarity in load distribution factors, obtained for the respective superloads in the next section. The above conclusions can also be extended to the third and fourth superloads, based on the results presented in Figures12a and 12b for those two loads.

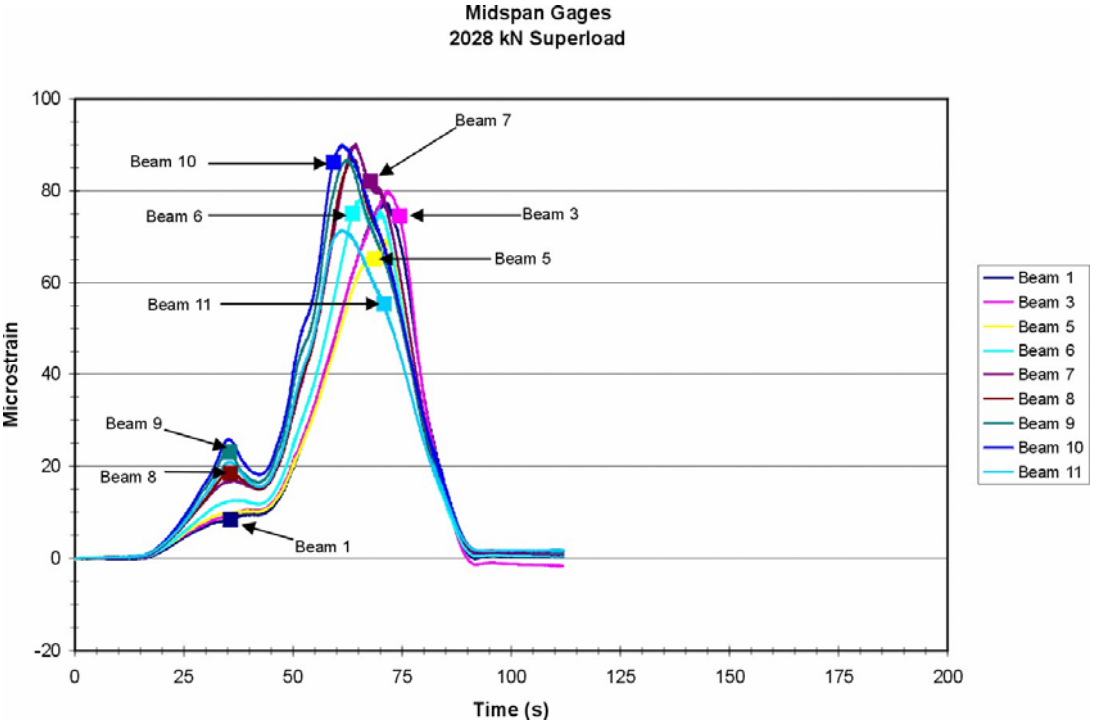

a. First superload: Crossed crabbed.

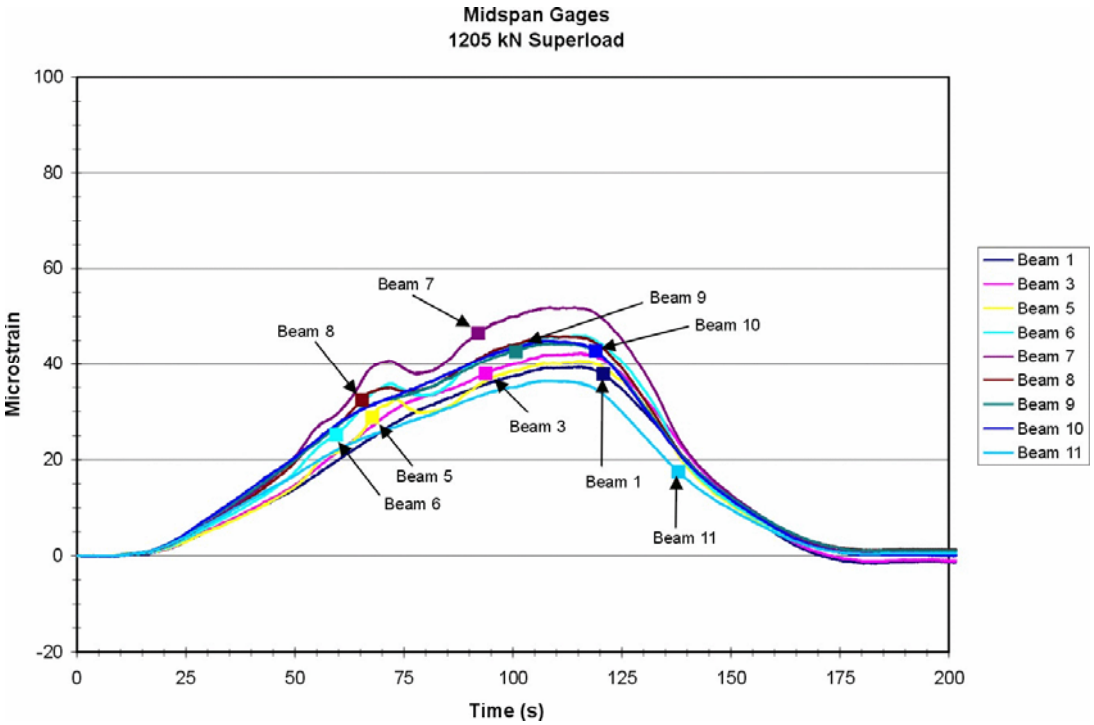

b. Second superload: Crossed diagonally.

Figure 11. Strain histories for the January 28, 2002 superloads.

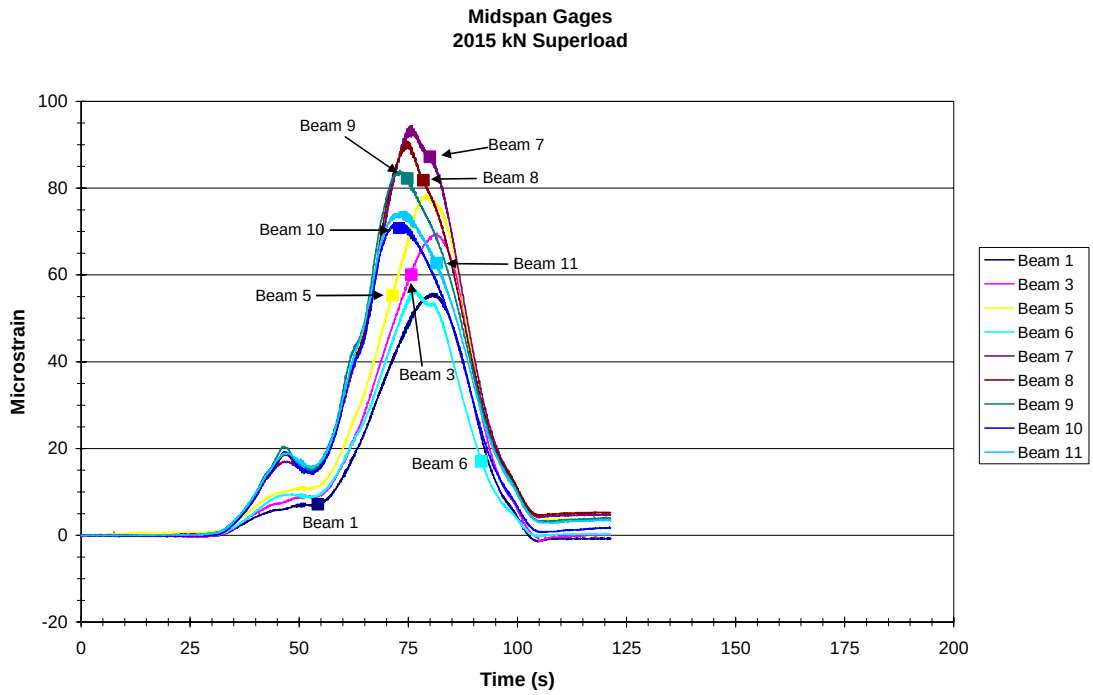

a. Third superload: Crossed crabbed.

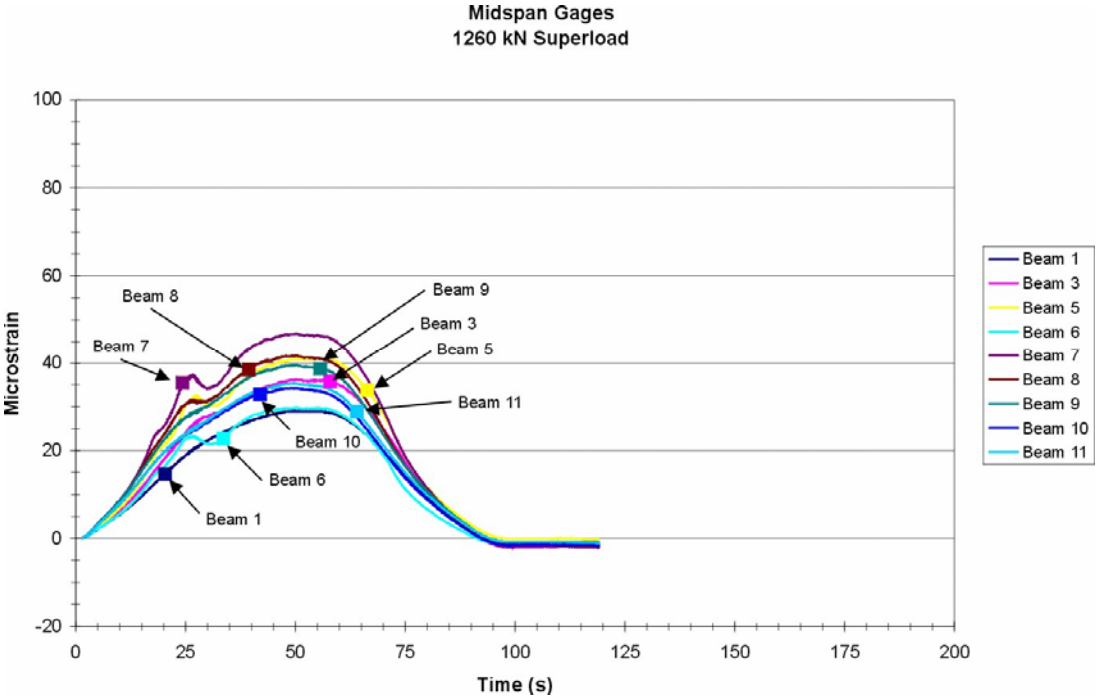

b. Fourth superload: Crossed diagonally.

Figure 12. Strain histories for the March 6, 2002 superloads.

B. TRANSVERSE LOAD DISTRIBUTION

Figures 13a and 13b, and 14a and 14b, respectively, show the load distribution plots for the first and second, and third and fourth superload trucks, calculated at various times during a superload crossing. The dotted heavy lines in these plots correspond to time instances when the loaded trailers were centered about the bridge midspan. A load distribution factor is defined here as the percentage of the superload total moment carried by a beam, at any time during the slow superload crossing of the bridge. These figures also show the variation in load distribution factors for selected times during a superload crossing and good load distribution when the superload effect was maximum on the bridge. The dotted heavy lines in Figures 13a and 13b, which correspond to the times when the strains peaked in Figures 11a and 11b, clearly demonstrate similarity in transverse load distribution under the two crossing patterns. The above conclusions can also be extended to the third and fourth superloads, based on the results presented in Figures 12 and 14 for these two loads. Note that the distribution factors determined in this report for the two crossing patterns (about 0.12 of the total truck moment) are lower than those commonly used in line girder analysis, which can be obtained based on the AASHTO Standard Specifications (0.66) or the AASHTO Guide Specification for Load Distribution (0.55) *(6, 8)*.

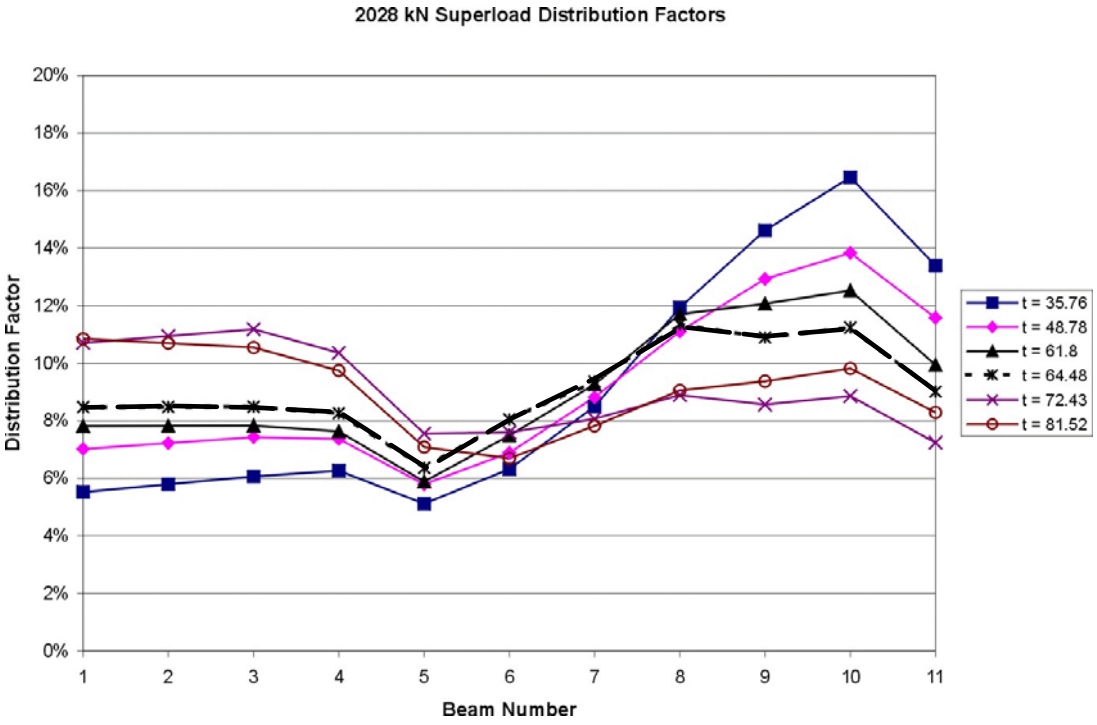

a. First superload: Crossed crabbed.

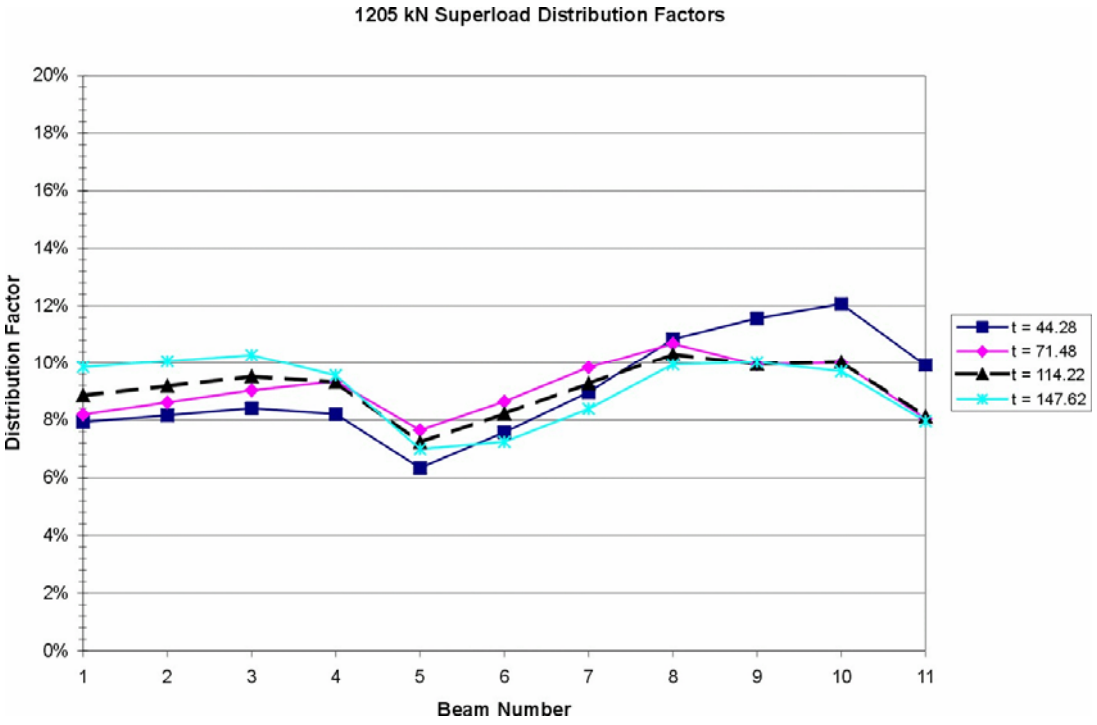

b. Second superload: Crossed diagonally.

Figure 13. Transverse load distribution for the January 28, 2002 superloads.

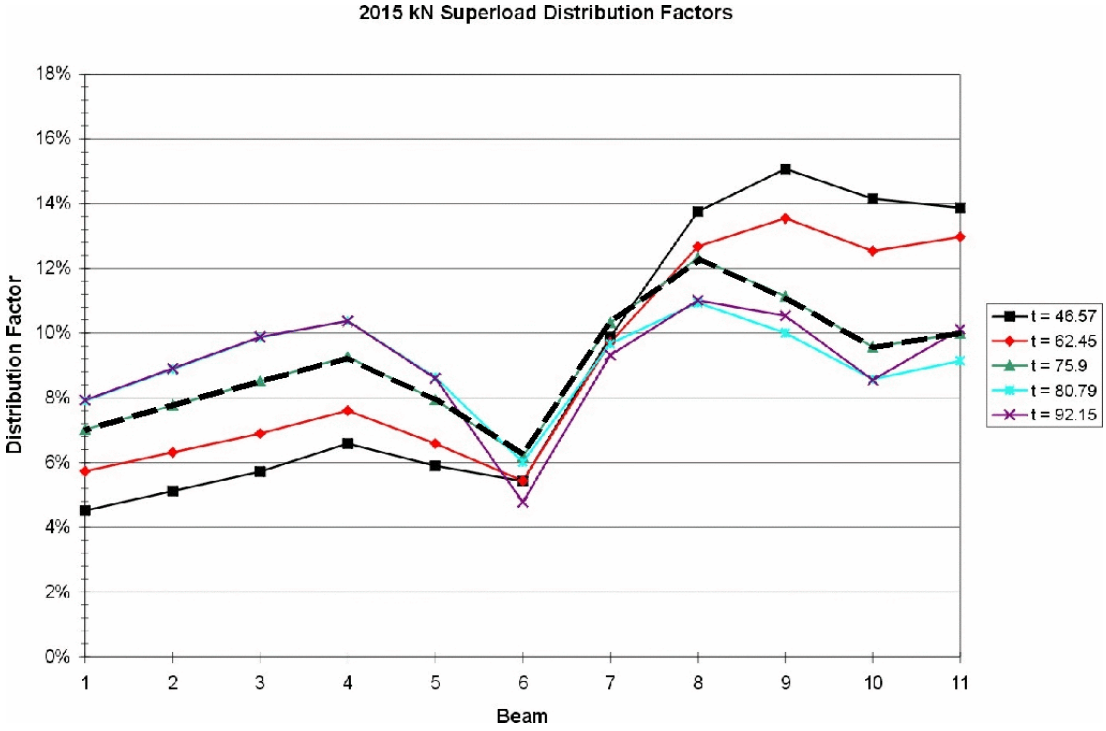

a. Third superload: Crossed crabbed.

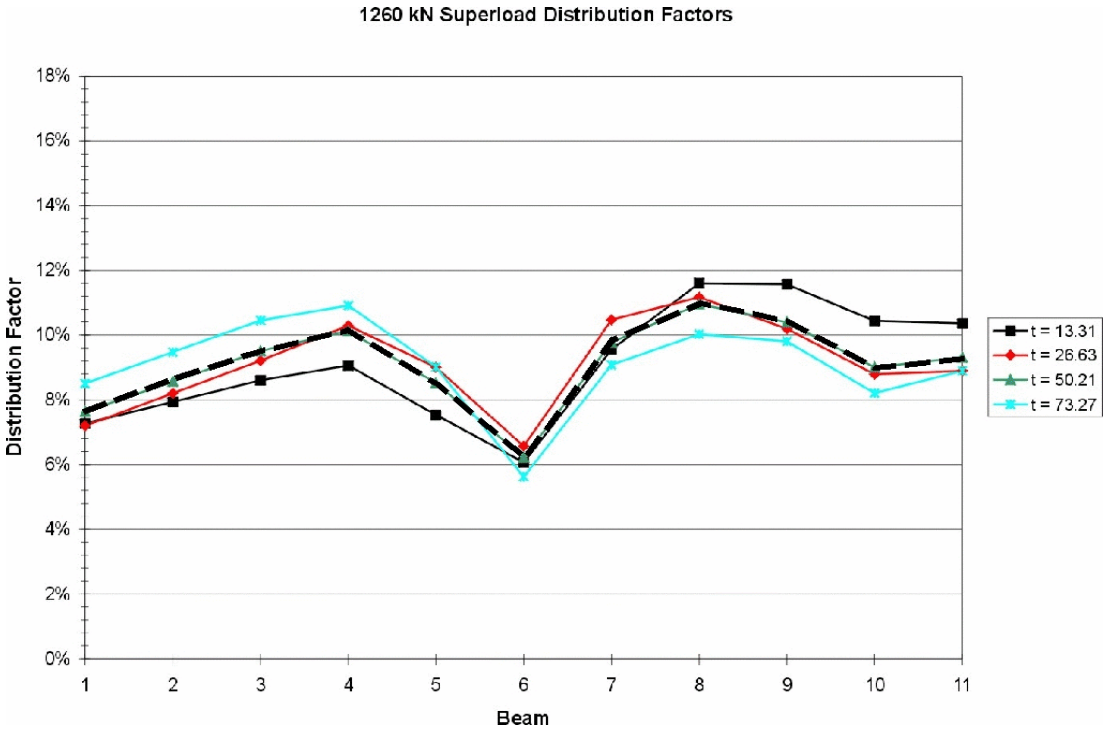

b. Fourth superload: Crossed diagonally.

Figure 14. Transverse load distribution for the March 6, 2002 superloads.

C. BEAM 11 INVESTIGATION

Strain data from the three gages mounted on the side of Beam 11 (Figure 15) were used in this investigation. The investigation is limited to the strain histories recorded for the first and second superloads in Figures 16a and 16b, respectively. Using this data and the calculated distribution factors in the previous section, neutral axis locations, measured from the beam bottom, and moments carried by Beam 11 can be determined. These locations and moments can be obtained, respectively, for the first superloads as 76.2 cm (30 in.) and 4.95 x 10^5 N-m (365 kip-ft), and for the second superload as 76.2 cm (30 in.) and 2.63 x 10^5 N-m (194 kip-ft). The ratio between the calculated moments (1.88) is very close to the ratio between the loaded trailers' weights (1.68), which supports the conclusion reached in the previous section when comparing the two crossing patterns.

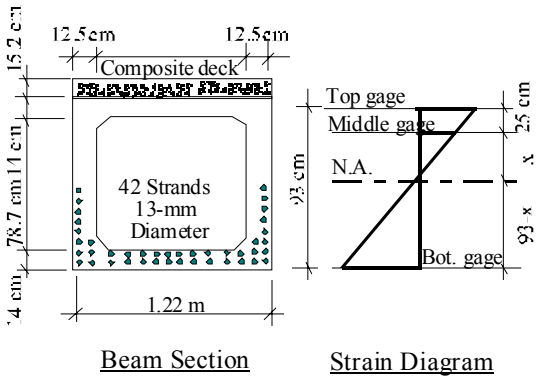

Figure 15. Beam 11 gages.

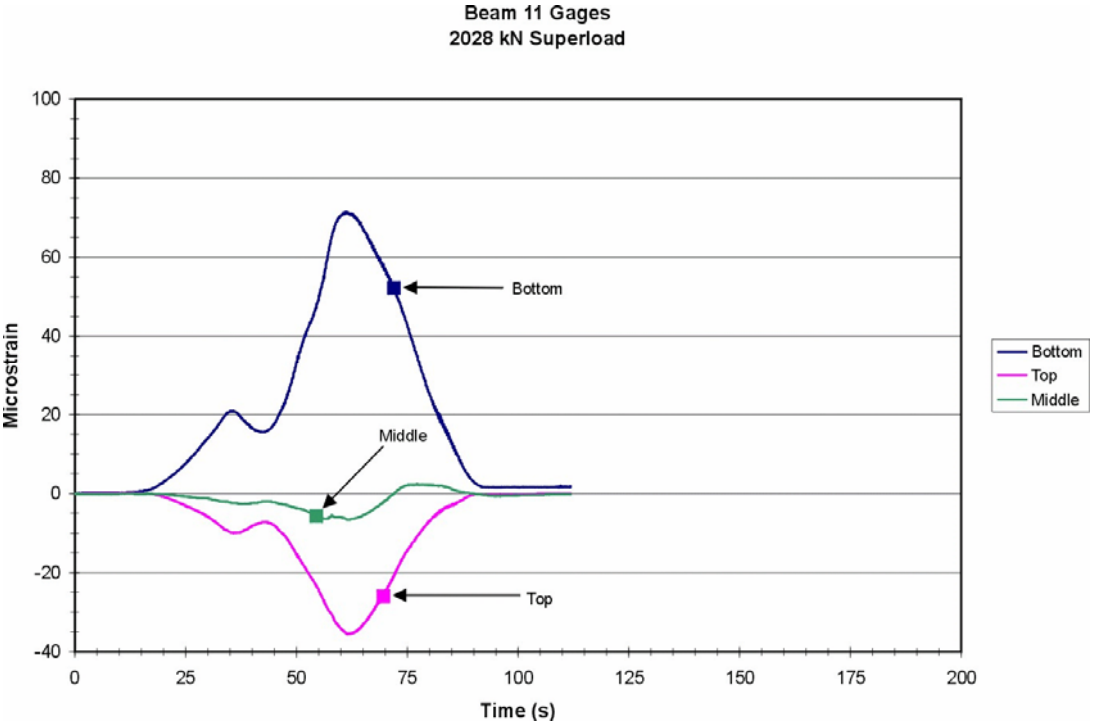

a. First superload: Crossed crabbed.

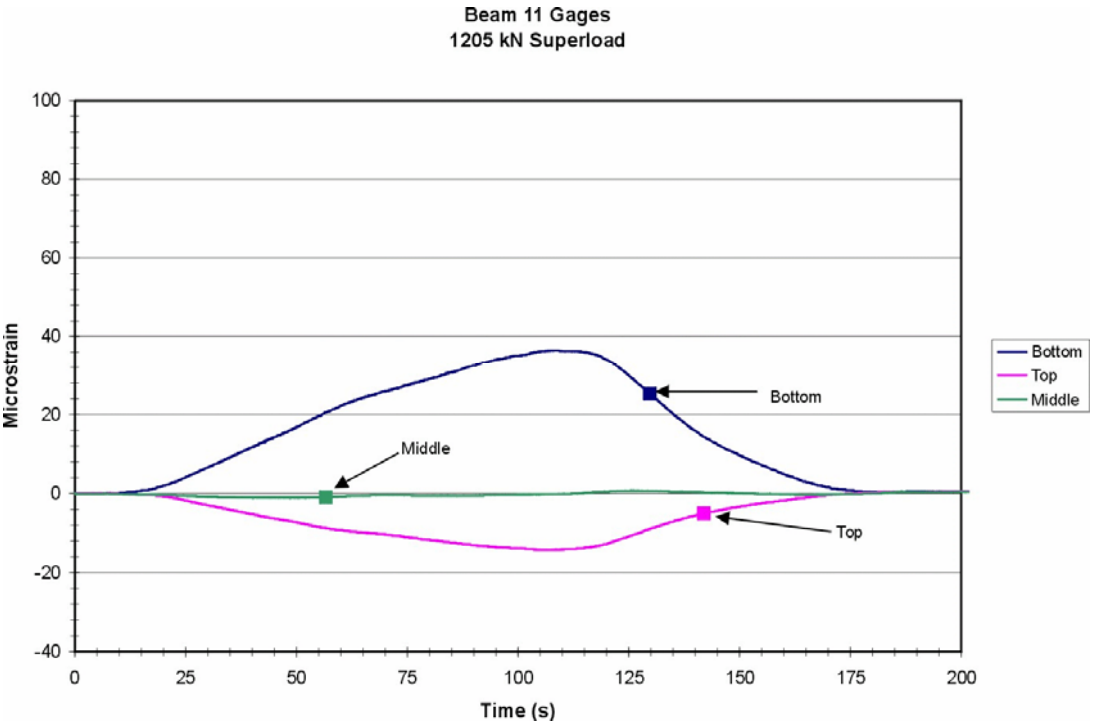

b. Second superload: Crossed diagonally.

Figure 16. Beam 11 strain histories for the January 28, 2002 superloads.

D. CONCRETE STRESSES

BRADD-2, Bridge Automated Design and Drafting Software, was used to determine total tensile stresses in the concrete at midspan of Beams 7 and 8, two of the most stressed beams. These stresses are plotted against the actual moment on the bridge in Figure 17. The figure shows 2 vertical lines, representing the dead load moment and the moment that would cause cracking of the beams, two inclined lines, and labeled moment stress points. In this figure, the dashed line, labeled "Actual," represents the moments and stress levels in the beam due to dead load and superload. The solid line, labeled "Simply Supported," represents the moment and stress levels in the beam due to dead load and superload, with the superload moments calculated analytically using the developed program simply supported solution. The small box labels, "Adjusted SS," represent the moments and stresses for selected superloads, obtained by multiplying the simply supported moments by a factor (0.52 to 0.66) determined using the developed program. This factor reflects the effect of the integral abutments in reducing the beam's simply supported moment. From Figure 17, it is clear that the moment in the bridge beams induced by the crossing superloads remained well below the cracking moment.

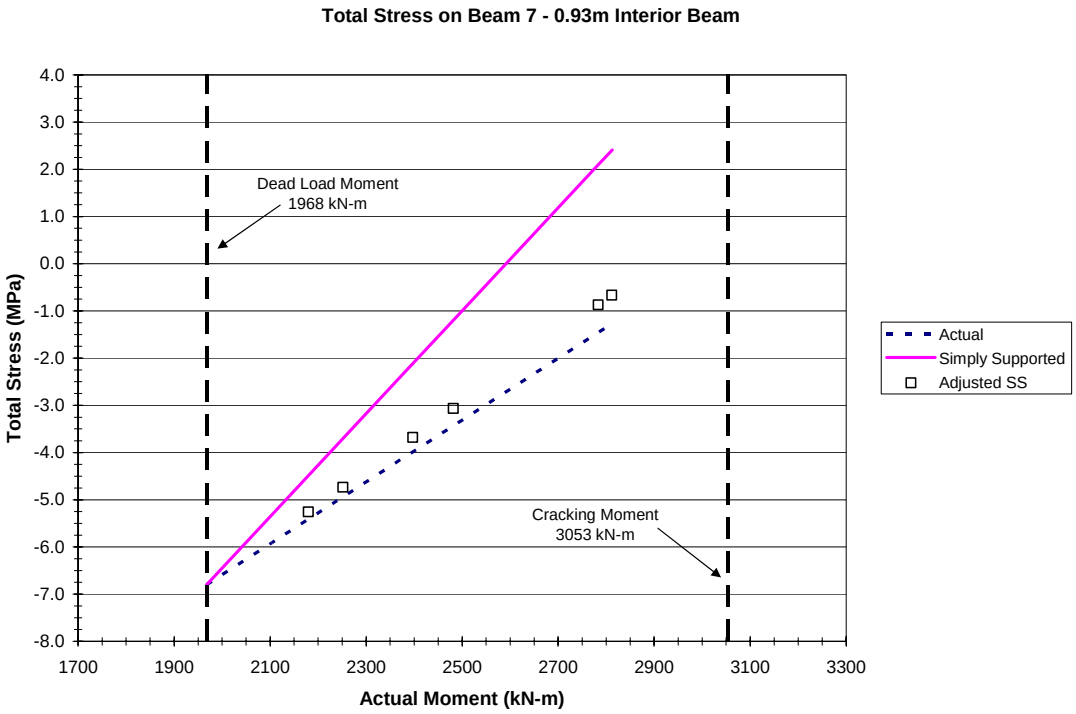

a. Beam 7 stresses.

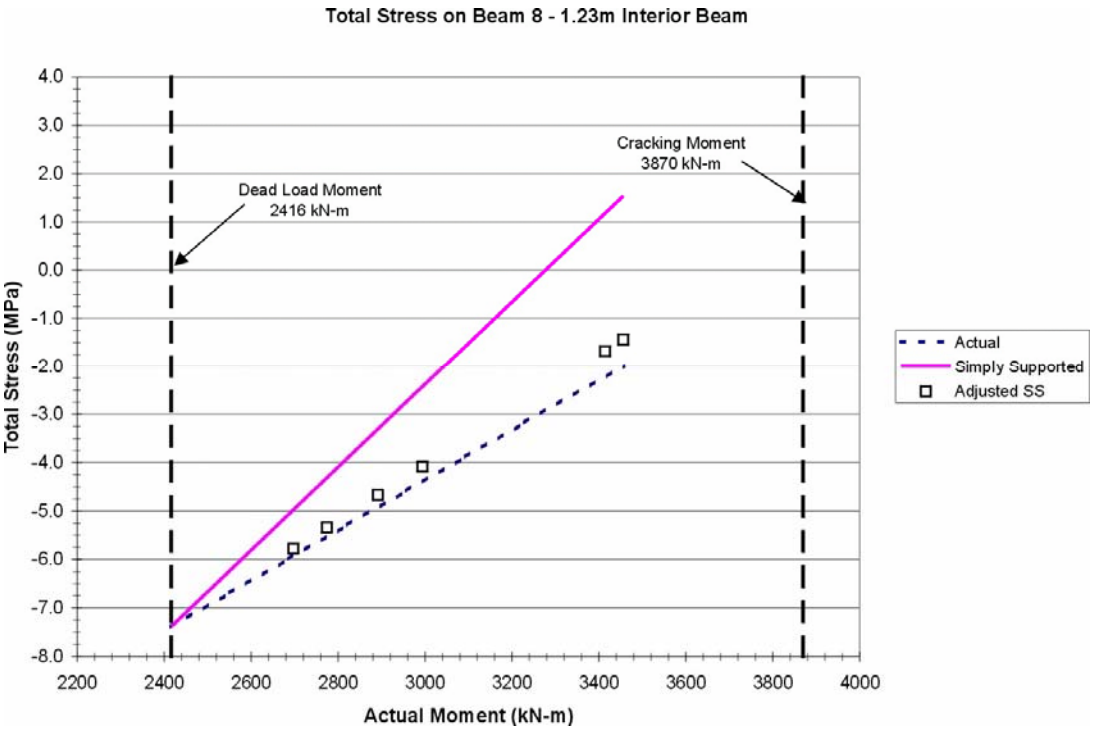

b. Beam 8 stresses.

Figure 17. Beams 7 and 8 total stresses.

E. END FIXITY INVESTIGATION

The effect of this fixity is clearly demonstrated by Beam 8 strain histories in Figures 18 and 19, noting the negative bending experienced by the beam near the abutments. Similar bending was observed for the strain history results for the first and second superloads *(9)*. This end fixity is further illustrated in Figure 20 which compares actual midspan bridge moment for the third superload (2015 kN) to those calculated assuming simply supported and fixed end conditions. From this figure, it can be concluded that the structure behaved somewhere between being simply supported and completely fixed. Limited analysis on this beam, because of computational difficulty, showed excellent agreement between actual/measured and calculated fixed-end moments and shears.

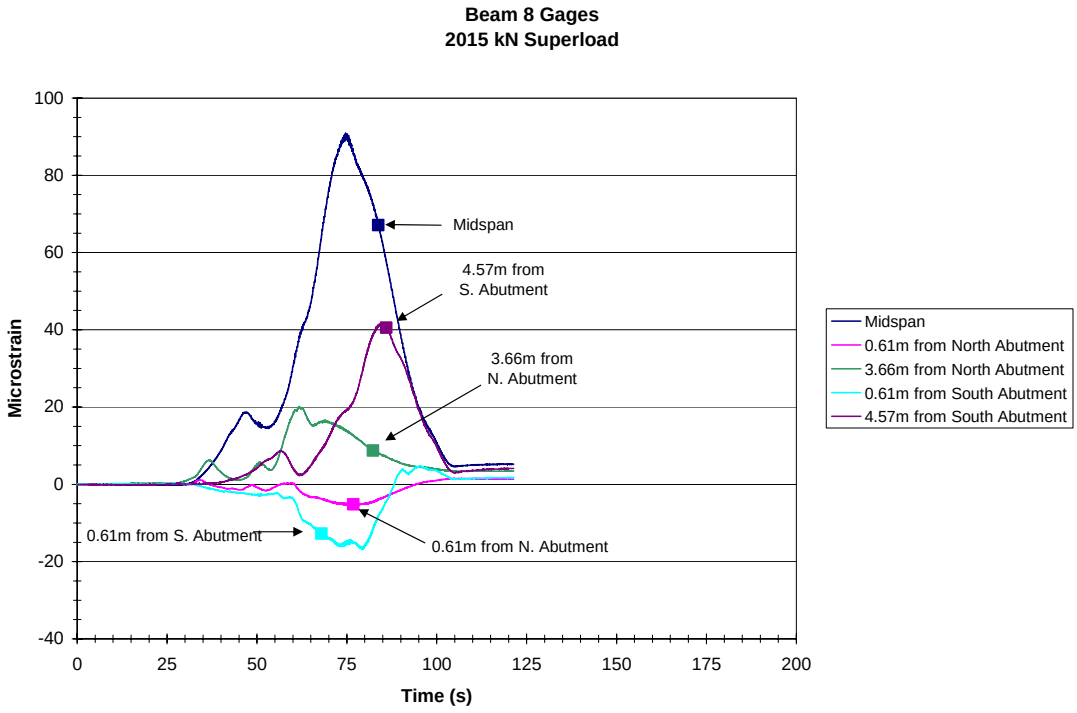

Figure 18. Beam 8 strain history for the third superload.

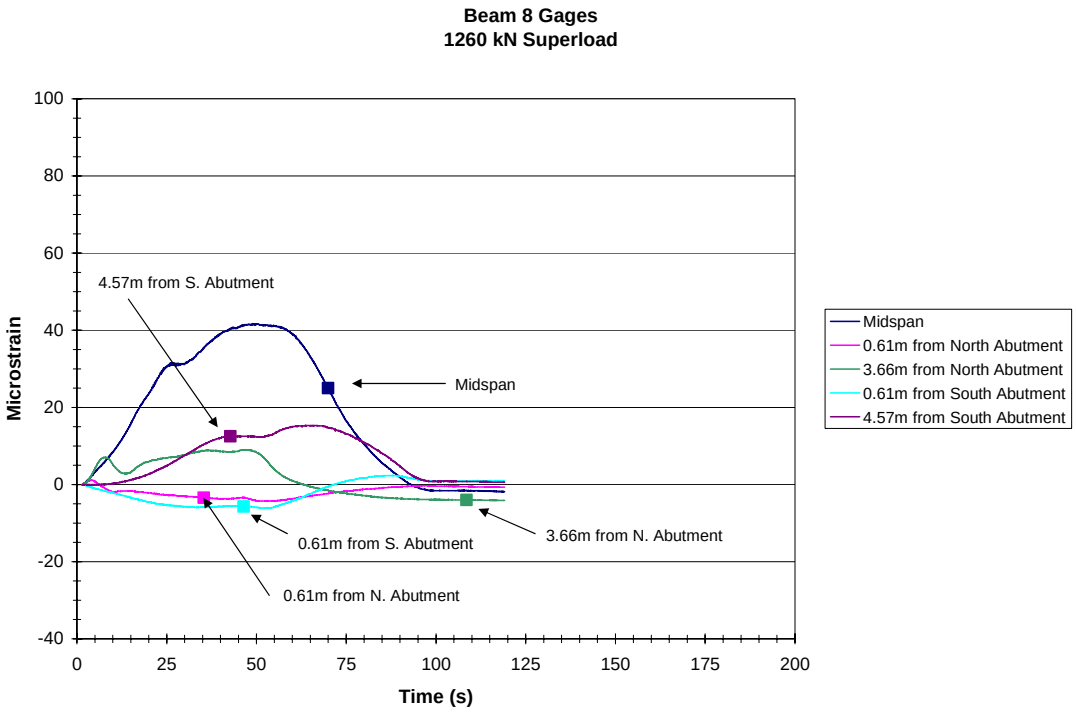

Figure 19. Beam 8 strain history for the fourth superload.

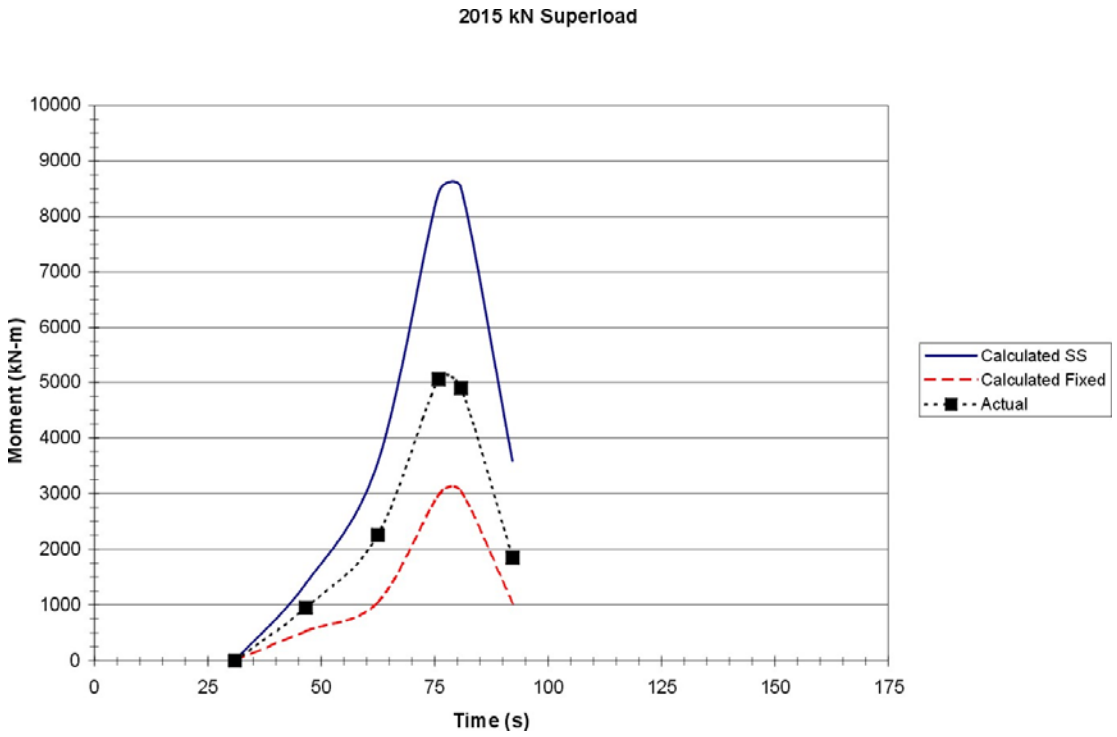

Figure 20. Moment comparison for the third superload: Crossed crabbed.

V. LOAD TESTS RESULTS AND DISCUSSIONS

A. STRAIN HISTORIES

The strain histories for the six load tests are shown in Figures 21 to 23. Load Tests 1 and 2 (Figure 21) resemble one lane loaded scenarios on the west and east lanes, respectively. The strain history results for these tests clearly show that the beams directly under the trucks wheel lines were stressed most (Beams 3 and 5 for Load Test 1, and Beams 7, 8, and 9 for Load Test 2). The highest recorded strains in the two tests were within 3 με, which may be attributed to a difference in the lead distance between the two trucks as they crossed the bridge during the tests. The two time histories did not mirror image each other because the readings for the gages on Beams 2 and 4 were linearly interpolated, using neighboring gage readings.

Load Tests 3 and 4 (Figure 22) were intended to maximize the load on the east and west fascia beams, respectively. The strain history results for these tests, again show that most of the load was carried by Beams 7 to 11, and 1 to 5, for Load Tests 3 and 4, respectively. The highest recorded strains during the two tests were within 6 με, which may be attributed to a difference in the lead distance between the trucks during the crossing.

The strain histories for Load Tests 5 and 6 in Figure 23 represent the two trucks in side by side formations, moving at a crawl speed (Load Test 5) and statically positioned at the bridge midspan (Load Test 6). The strain history results for the two tests show that Beams 3 to 5 and 7 to 9 were the most stressed, with the highest strains in the two tests within 4 με.

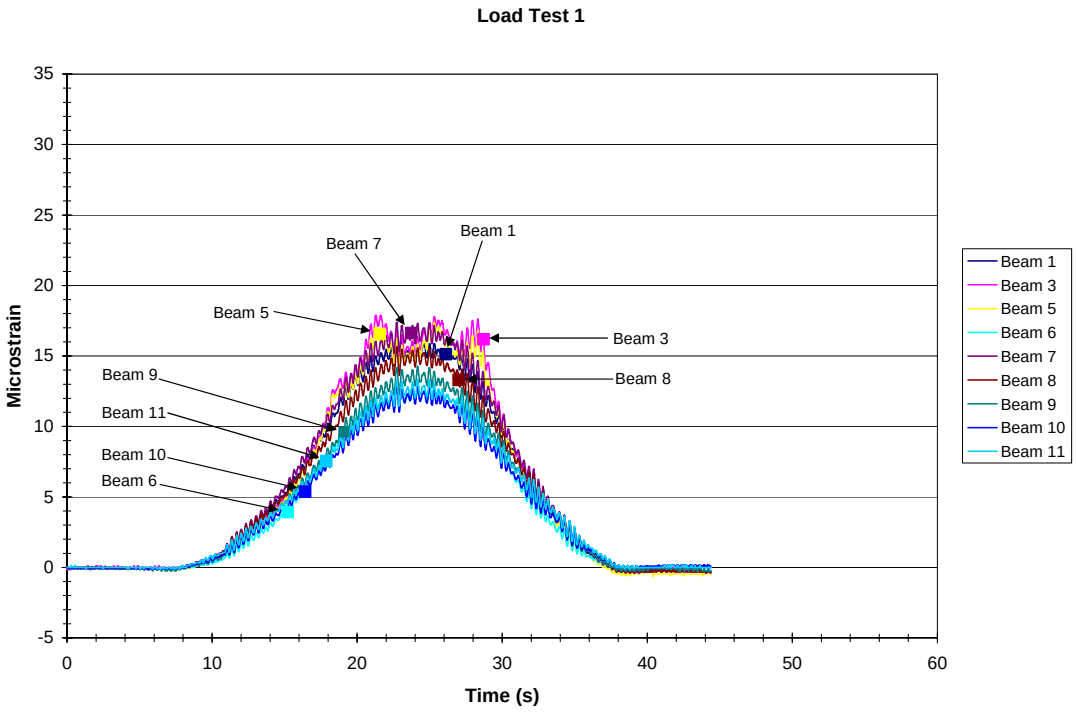

a. Test trucks crossing at crawl speed in the west lane.

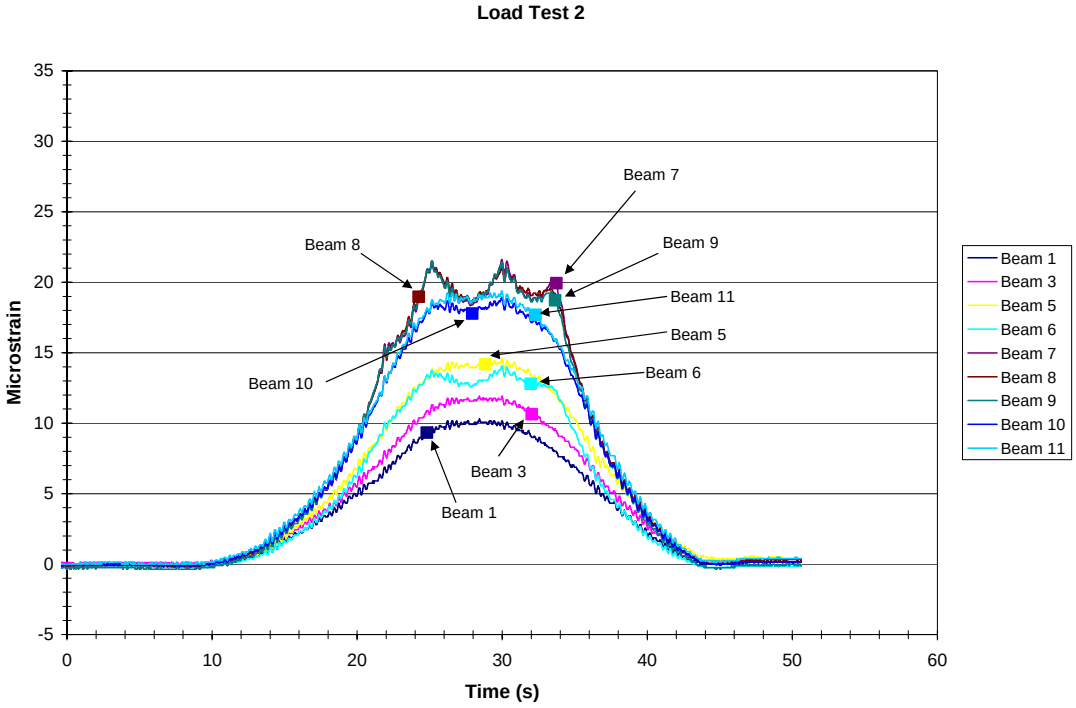

b. Test trucks crossing at crawl speed in the east lane.

Figure 21. Load Tests 1 and 2 strain histories.

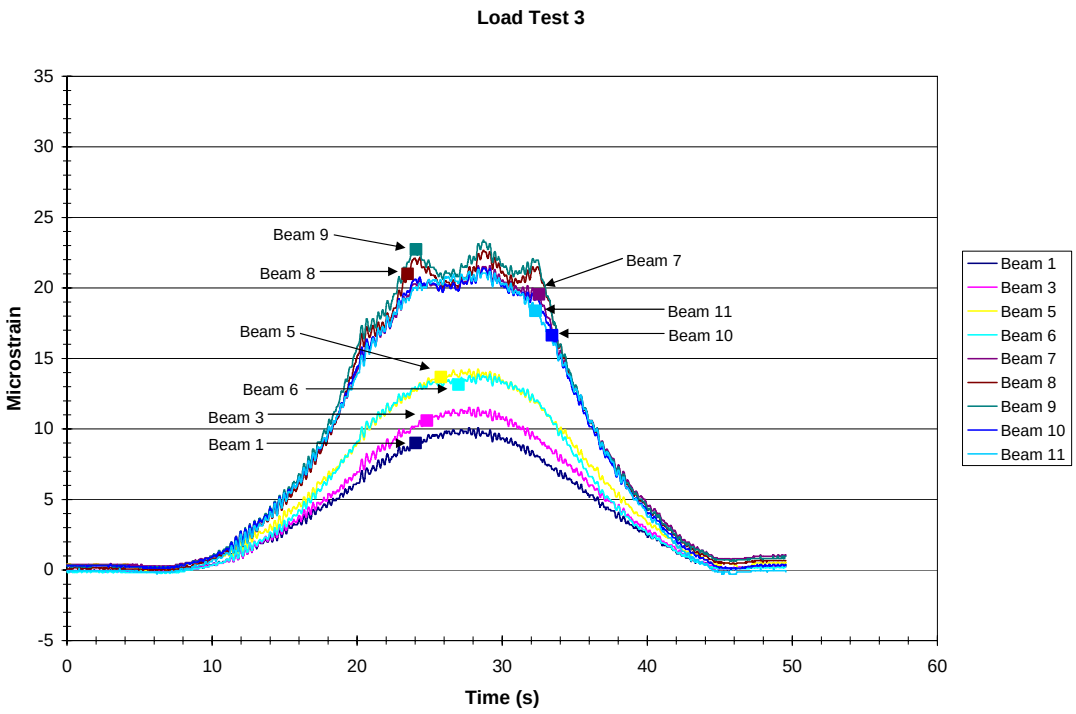

a. Test trucks crossing at crawl near the east fascia beam.

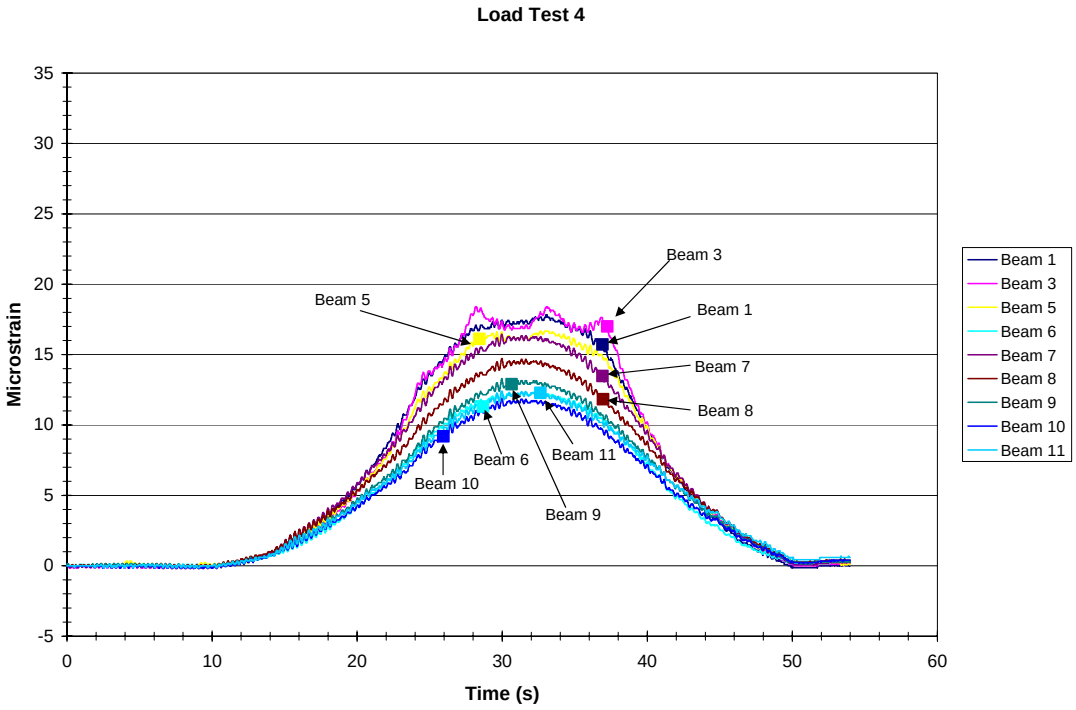

b. Test trucks crossing at crawl near the west fascia beam.

Figure 22. Load Tests 3 and 4 strain histories.

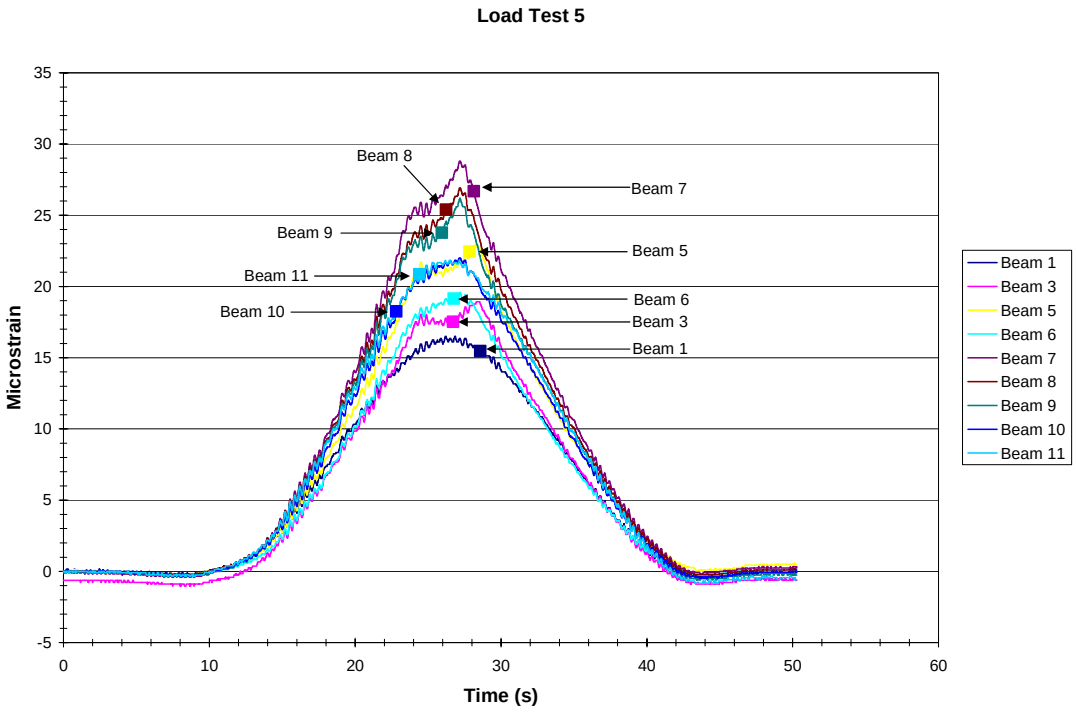

a. Test trucks crossing side by side at crawl speed down the bridge center line.

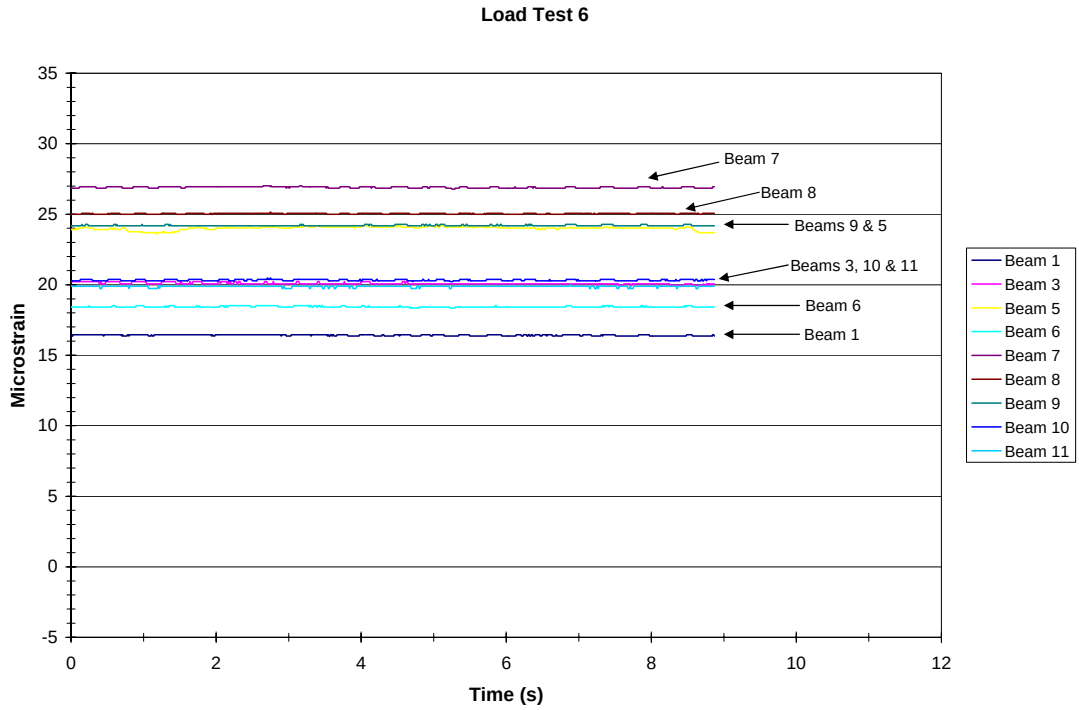

b. Test trucks statically positioned side by side at the bridge midspan.

Figure 23. Load Tests 5 and 6 strain histories.

B. TRANSVERSE LOAD DISTRIBUTION

Transverse load distribution plots are shown in Figures 24 to 26. The plots, generally, show expected symmetry and anti-symmetry trends. The one lane truck loadings resulted in a distribution factor of about 12 percent. The highest transverse load distribution factor (about 14 percent) was obtained for Load Test 3, the test maximizing the load applied on the east fascia beam (Figure 10).

C. LOAD DISTRIBUTION COMPARISONS

Some of the results derived from the strain histories for the load tests and two of the superload moves are summarized in Tables 3 and 4. Noting the crossing times and the times to maximum strains in the tables, it can be concluded that the maximum strain times are consistent with the instances maximizing the loading at the bridge midspan. For Load Test 5, for example, the maximum moment/strain is obtained when the back axles are at the bridge midspan, and for the superloads, when the trailer carrying the superload is centered about the bridge midspan. Those are reflected in the highest strains occurring during the second halves of the crossing times. The tables also show that the highest distribution factors obtained during the load testing and superload crossing were very similar (about 14 percent). This is an important finding, noting the differences in crossing patterns and crossing load size and location.

Test	Test Focus	Crossing Time (s)	Time to Maximum Strain (s)	Maximum Strain (με)	Highest Distribution Factor (%)
1	West Lane	30	14	17	12
2	East Lane	32	14	21	14
3	East Fascia	36	16	23	14
4	Wast Fascia	38	16	18	12
5	Center Beams	32	18	28	12
6	Center Beams	NA	NA	26	12

Table 3. Load test results summary.

Test	Test Focus	Crossing Time (s)	Time to Maximum Strain (s)	Maximum Strain (με)	Highest Distribution Factor (%)
First Superload	All Beams	75	47	90	11
Second Superload	All Beams	155	100	56	14

Table 4. Superload monitoring results summary.

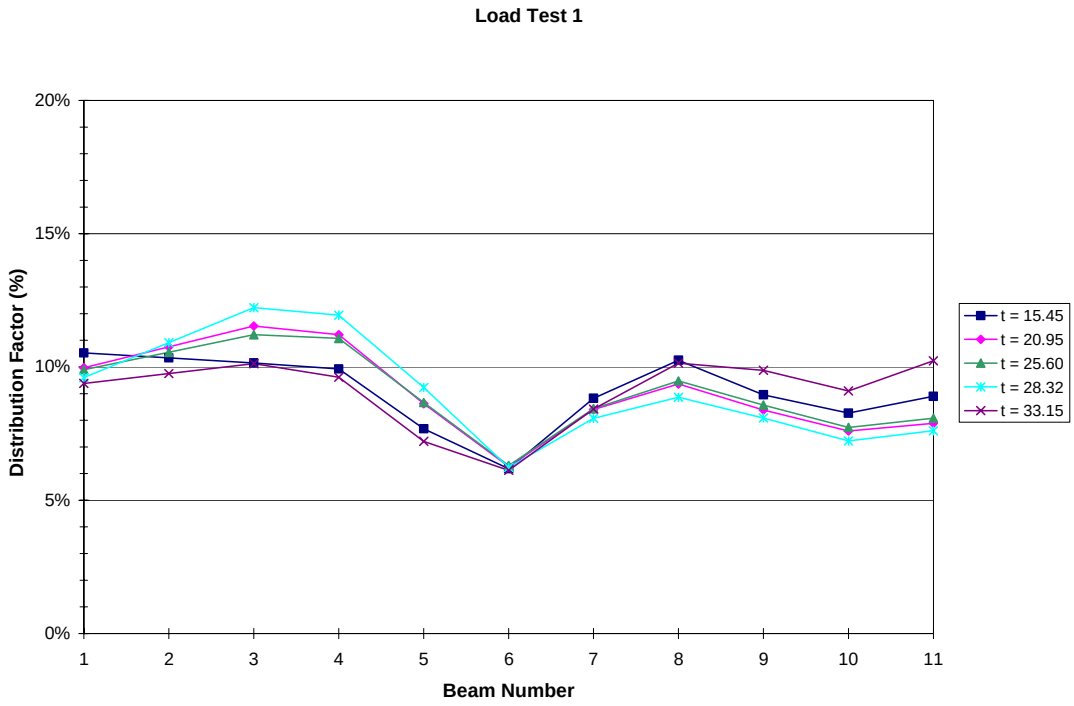

a. Test trucks crossing at crawl speed on the west lane.

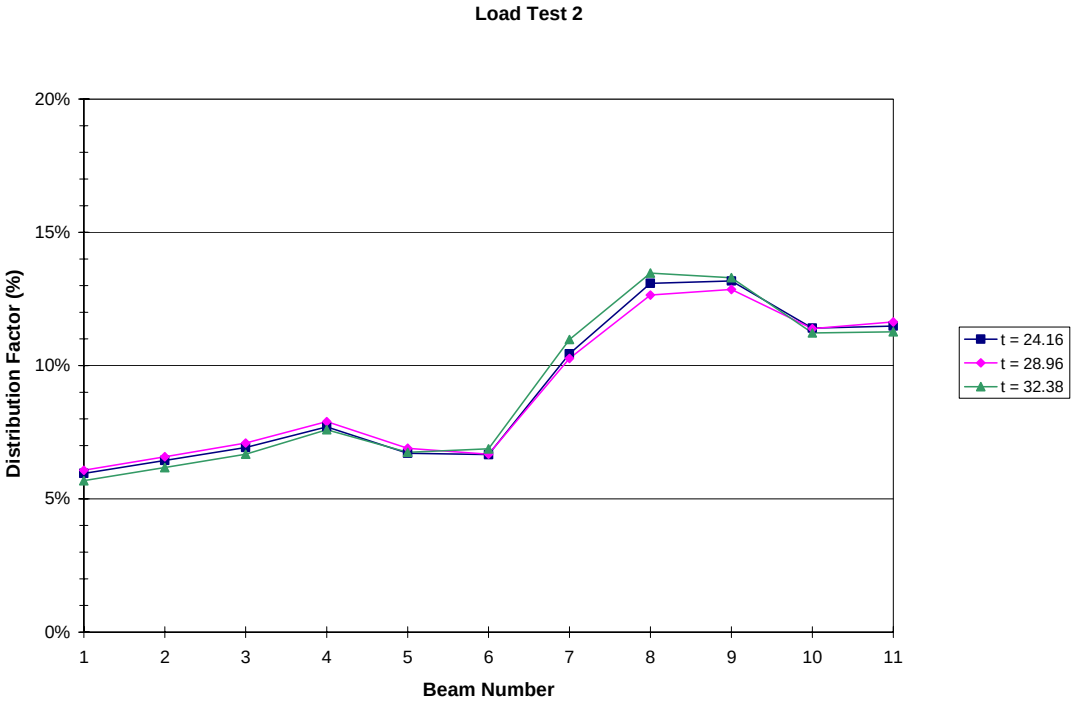

b. Test trucks crossing at crawl speed on the east lane.

Figure 24. Transverse load distribution for one lane truck loading.

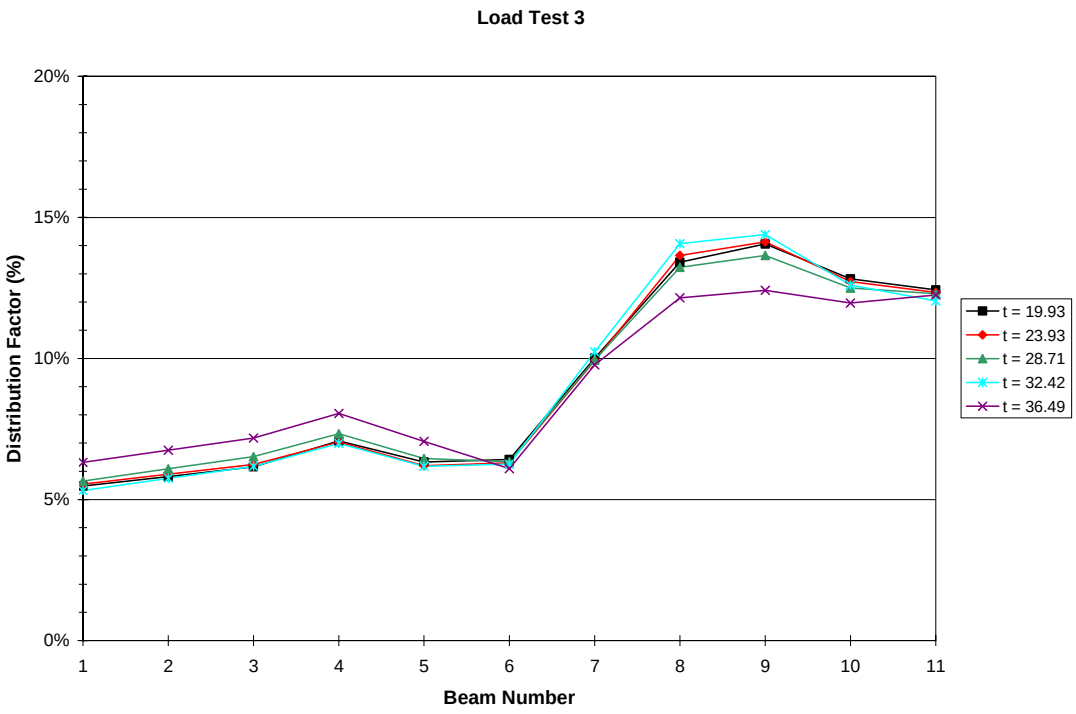

a. Test trucks crossing at crawl speed near the east fascia beam.

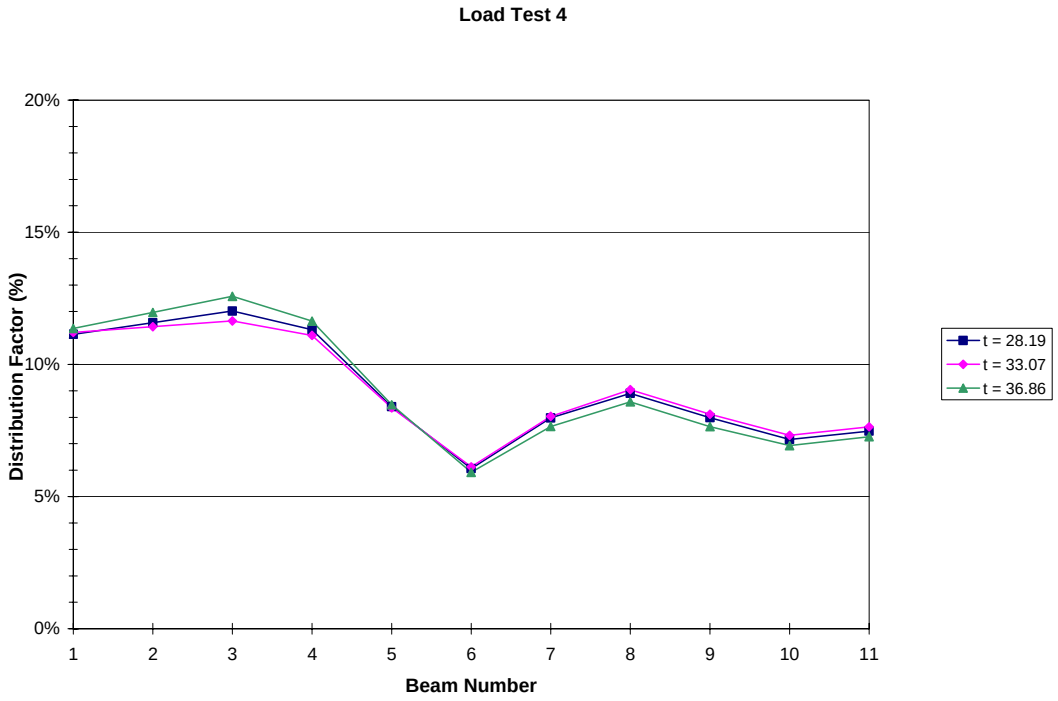

b. Test trucks crossing at crawl speed near the west fascia beam.

Figure 25. Transverse load distribution for fascia beam truck loading.

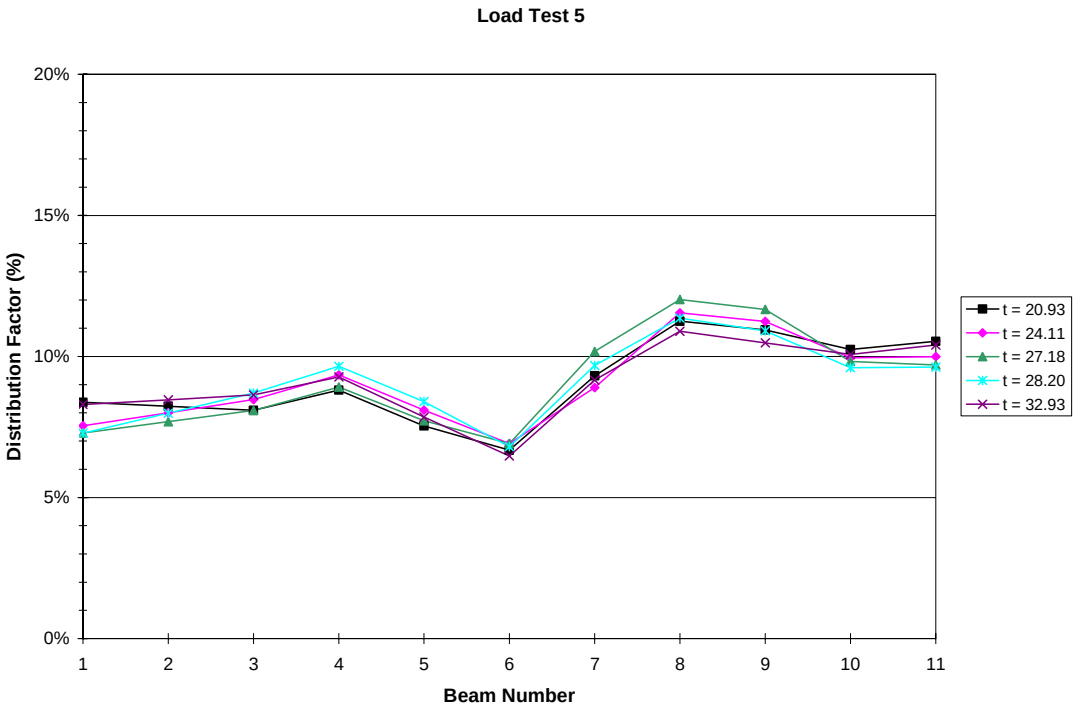

a. Test trucks crossing side by side at crawl speed down the bridge center line.

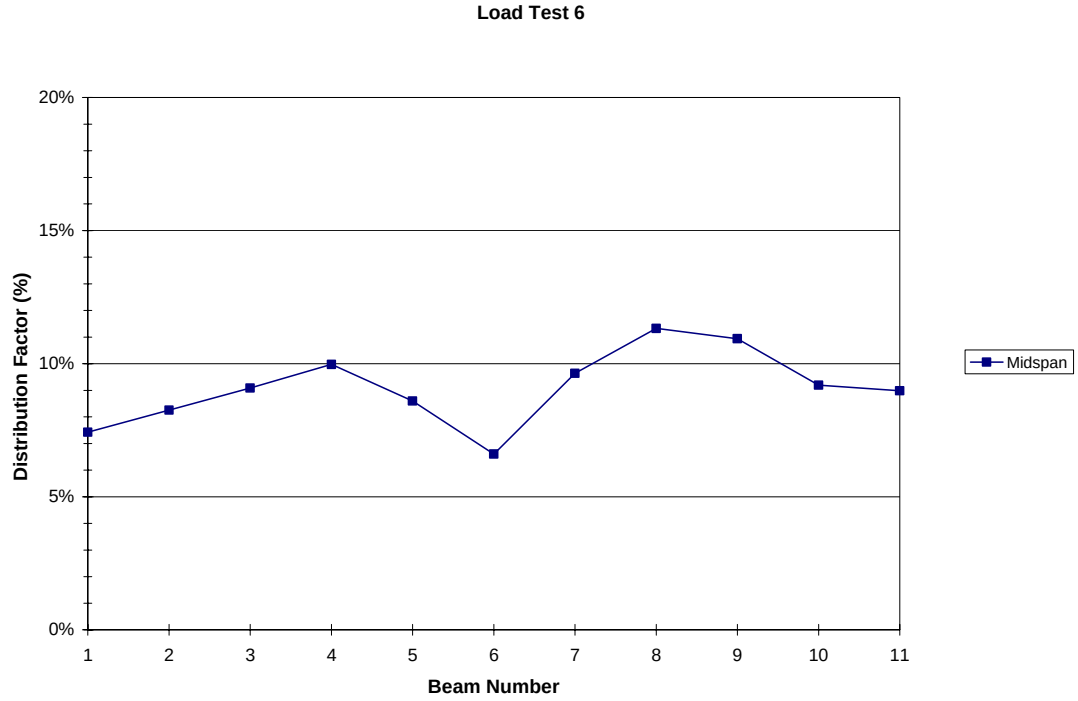

b. Test trucks statically positioned side by side at the bridge midspan.

Figure 26. Transverse load distribution for side by side formation truck crossing.

D. BEAM 11 INVESTIGATIONS

Beam 11 strain histories during Load Tests 3 and 5, the tests with the highest strains, are shown in Figure 27. These time histories may be compared with those in Figure 16 for the first and second superloads. Beam 11 results obtained using the strain histories for the two superloads and the two load tests are summarized in Table 5. For this beam, the table shows the maximum stresses, distribution factors, neutral axis locations, and midspan moments assuming both simply supported (SS) and fixed end (FE) conditions for the four loading scenarios. The highest stress in the beam due to the superloads is about 3.4 times that obtained during the testing. This ratio may be compared to that obtained by dividing the weight of the trailer carrying the superload by the weight of the two test trucks (4.3). The difference between the two is attributed to the crossing pattern. The neutral axis locations obtained under the four loading scenarios are very similar, with an average location of about 752 mm (29.6 in.), measured from the bottom of the beam. This location is higher than that calculated, theoretically, assuming an effective concrete deck thickness of 152 mm (6 in.) [648 mm (25.5 in.)]. Each of the three moments in the table is plotted against the stress column in Figure 28 to obtain a section modulus. A test-based modulus, given by the slope of the "Test" line in the figure [(0.2127 m^3) (12960 $in.^3$)], is comparable to the theoretical modulus of 0.1931 m^3 (11766 $in.^3$). From the figure, it is clear that the section modulus obtained as the slope of either of the SS or FE lines would not compare that well with the theoretical section modulus (SS would overestimate and FE would underestimate the section modulus). These findings support the previously stated conclusion on the structure's end conditions, being somewhere between simply supported and completely fixed.

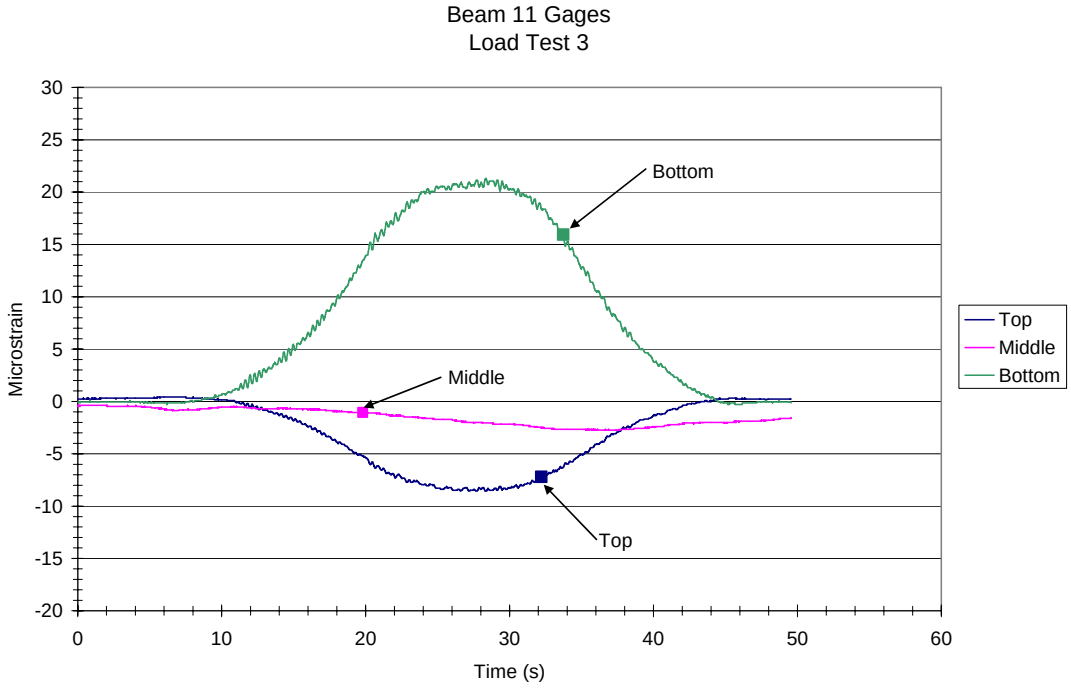

a. Load Test 3 results.

Figure 27. Beam 11 strain histories for Load Tests 3 and 5.

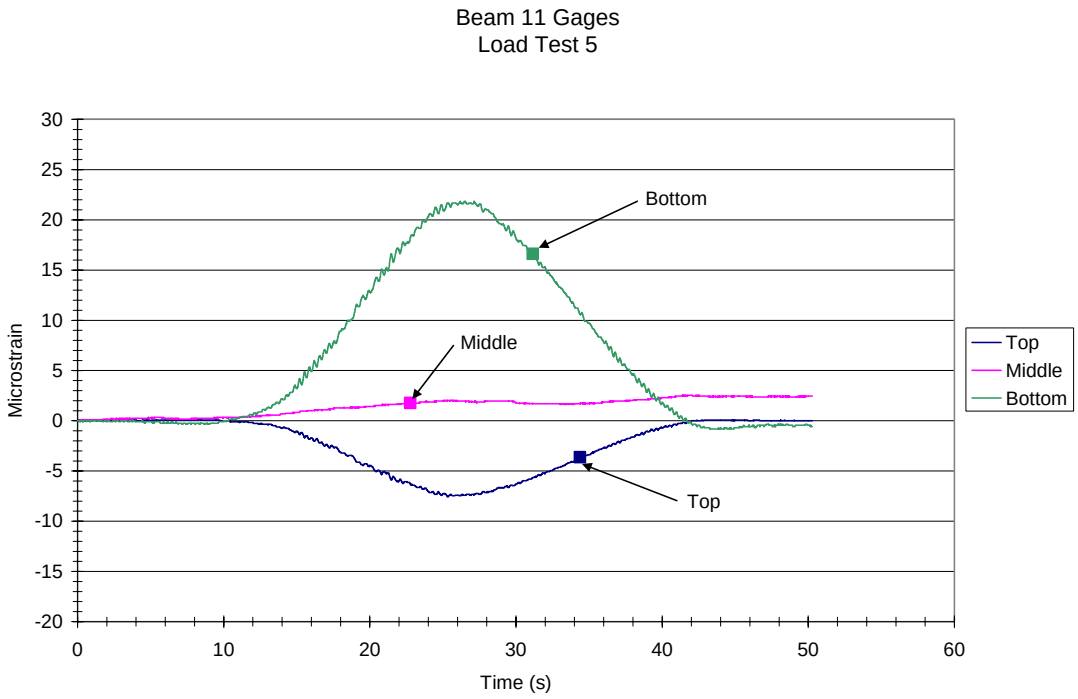

b. Load Test 5 results.

Figure 27. Beam 11 gages strain histories for Load Tests 3 and 5 (Continued).

The data in Table 5 was used to generate the plot in Figure 29. From this figure, the actual AASHTO distribution factor based on the test results can be obtained as 0.43. This factor may be compared to those in Chapter IV, which were calculated based on the AASHTO Standard Specifications (0.66) and the AASHTO Guide Specification for Load Distribution (0.55) *(6, 8)*. It is important to note that the "Test" linear fit lines, with high "R" values, in Figures 28 and 29 clearly demonstrate linear behavior of the structure during the monitoring and load testing. This supports the conclusion, made earlier in the report (Figure 17), that the total moment on the structure during the superload moves remained below that which would cause cracking of the beams.

Load Case	Stress (kPa)	Distribution Factor (%)	Neutral Axis Location (mm)	Moment (kN-m)		
				SS	FE	Test
First Superload	2413	11%	729	956	344	513
Second Superload	1227	10%	782	490	168	260
Test 5	752	13%	754	355	161	180
Test 3	717	11%	749	233	86	133

Table 5. Beam 11 results.

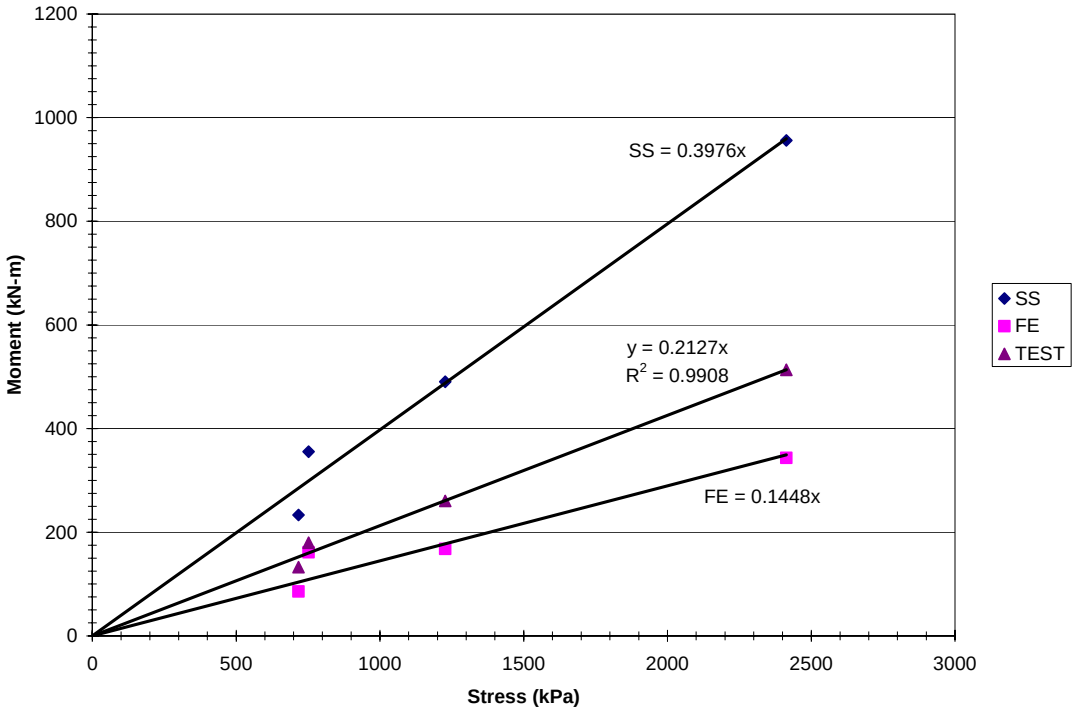

Figure 28. Beam 11 moment versus stress plots obtained based on simply supported (SS) and fixed end (FE) assumptions, and load test monitoring results.

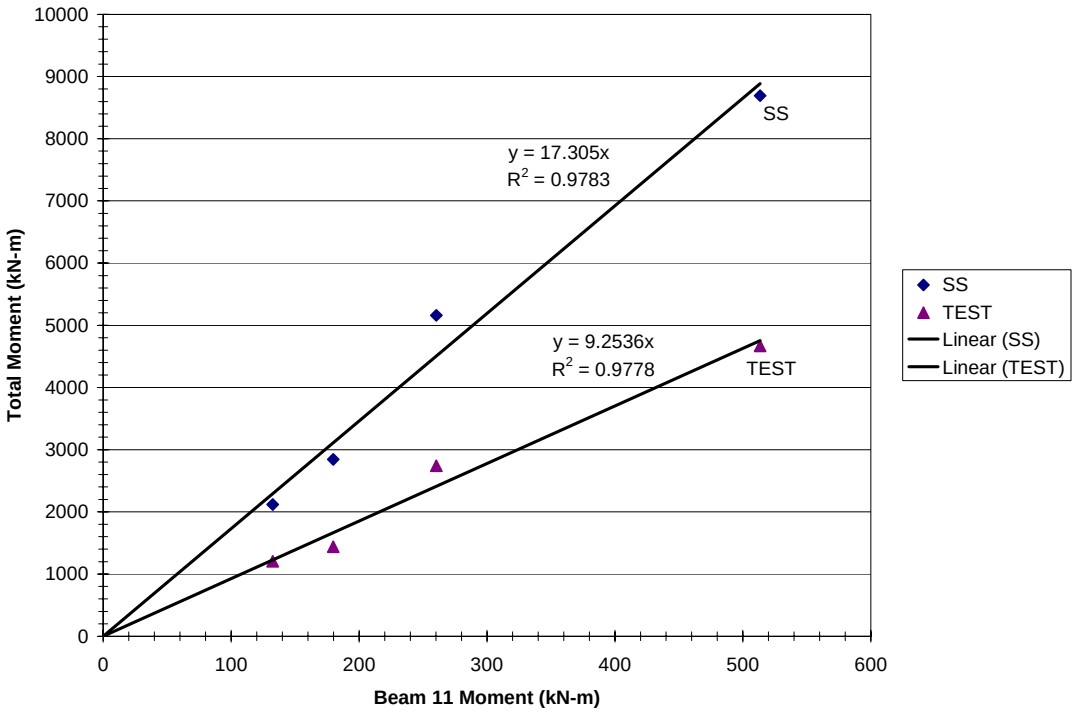

Figure 29. Total moment versus Beam 11 moment obtained based on simply supported (SS) assumptions and load test monitoring results.

VI. CONCLUSIONS

The report discussed monitoring and structural integrity evaluation of Coeymans Creek Bridge, South of Albany, NY, for superloads which crossed the bridge in two configurations: crabbed and driven diagonally. For this bridge, stress levels in the beams, did not show any clear advantages of crabbing over driving a superload diagonally across. This is a consequence to the similarity in the transverse load distribution results for the two crossing patterns. The monitoring results indicated very good transverse load distribution during the superload moves. With respect to midspan moments, the bridge acted somewhere between a completely fixed and a simply-supported structure. Live load moments on the bridge, computed based on the monitoring results, ranged from 52 to 66 percent of those calculated assuming a simply-supported structure. Additional analysis indicated that total bottom flange stresses at midspan due to the superloads were lower than those that would be required to cause cracking of the beams. Additionally, six load tests, using two trucks of known weights and configurations, were conducted to further investigate the behavior of the structure. The results from this testing confirmed the structure's end fixity, and, when compared with the results from this superload monitoring, provided very interesting conclusions about the structure response to traffic load.

The following can be concluded from this project:

1. Repeatability of the results. The results for the two crabbed superload trucks were very similar, as well as those obtained for the two superload trucks driven diagonally across the bridge. Each pair of super load trucks had close weights and were driven by similar tractor trailer combinations.

2. With respect to stress levels in the beams, there are no clear advantages of crabbing over driving the superload diagonally across the bridge. This is a consequence to the fact that similar transverse load distribution resulted for the two crossing patterns. The load distribution plots (Figures 13 and 14) for both the crabbed and diagonal loadings compare very well.

3. The excellent transverse load distribution observed during monitoring of the superloads was also confirmed by additional load testing, using trucks of known weights and configurations crossing the bridge in a straight fashion.

4. Analysis of the various load case data indicated that actual/measured midspan moments are linearly related to the simply-supported and fixed-end cases moments. Those factors imply that, with respect to midspan moments, the bridge acted somewhere between a completely fixed and a simply-supported structure. Simply supported factors ranged from 1.52 to 1.94 meaning that the actual midspan moments ranged from about 52% to 66% of the calculated simply supported midspan moments. Fixed factors ranged from about 0.5 to 0.80. These factors indicate that the actual moments ranged from about 125% to 200% of the midspan moments calculated assuming fixed end conditions.

5. Limited analysis of Beam 8 data showed excellent agreement between actual/measured and calculated fixed-end moments and shears.

6. Using data from BRADD-2, total bottom stresses in the concrete at midspan due to the various live load cases (superloads and test trucks) were found to be lower than that would be required to cause cracking (actual moments on the structure are lower than the cracking moments).

7. The conducted load testing results confirmed that the structure's level of end fixity is somewhere between that of a simply supported and that of a completely fixed structure.

8. The combined superload monitoring load testing results indicated that the highest load distribution factor remained the same (about 14 percent), regardless of the magnitude of the load on the bridge or the crossing pattern.

9. Linear behavior of the structure was exhibited during both the monitoring and the load testing.

ACKNOWLEDGMENTS

Instrumentation and data collection for this project was conducted by George Schongar and Harry Greenberg of the Transportation Research and Development Bureau. Ryan Lund, also with the Bureau assisted in this project. Tom Moon, Wahid Albert, and Norbert Luft of NYSDOT Structures Division provided support information, guidance, and valuable comments during the course of the project. NYSDOT Region 1 staff members assisted with the testing and traffic control.

REFERENCES

1. Turner, A., and Aktan, AE, "*Issues in Superload Crossing of Three Steel Stringer Bridges in Toledo, Ohio*," Transportation Research Record No. 1688, pp. 87-96, 1999.

2. Aktan, AE, Turner, A., and Levi, A., "*Instrumentation, Proof testing and Monitoring of Three Reinforced Concrete Deck-on-Steel Girder Bridges Prior to, During, and After Superload*," Ohio Department of Transportation ,Report No. FHWA/OH-98/015, 1998.

3. Beilfuss, CW, "*Vehicle Route/Bridge Analysis System for Superload Permitting, Final Report*," Ohio Department of Transportation, Report No. FHWA/OH-93/003, 1992.

4. Moses, FG., "*Truck Weight Effects on Bridge Costs, Final Report*," Ohio Department of Transportation, Report No. FHWA/OH-93/001, 1992.

5. Hunt, V., Helmicki, A., "Field Testing and Condition Evaluation of a Steel-Stringer Bridge for Superload," *Proceedings of Structural Materials Technology: NDE/NDT for Highways and Bridges*, Cinicnnati, OH, September, 2002.

6. *"Standard Specifications for Highway Bridges,"* 1996 (16th edition), American Association of State Highway and Transportation Officials, Washington, D.C.

7. "*Manual for Condition Evaluation of Bridges*," 1994, American Association of State Highway and Transportation Officials, Washington, D.C.

8. "*Guide Specifications for Distribution of Loads for Highway Bridges,"* 1994 (16th edition), American Association of State Highway and Transportation Officials, Washington, D.C.